Journal of Medicinal Chemistry

Article

Structure-Activity Relationships of potent, targeted covalent inhibitors that abolish both the transamidation and GTP binding activities of human tissue transglutaminase

Abdullah Akbar, Nicole M.R. McNeil, Marie R. Albert, Viviane Ta, Gautam Adhikary, Karine Bourgeois, Richard L. Eckert, and Jeffrey W. Keillor

J. Med. Chem., **Just Accepted Manuscript** • DOI: 10.1021/acs.jmedchem.7b01070 • Publication Date (Web): 31 Aug 2017

Structure-Activity Relationships of potent, targeted covalent inhibitors that abolish both the transamidation and GTP binding activities of human tissue transglutaminase

Abdullah Akbar,[‡1] *Nicole M. R. McNeil,*[‡1] *Marie R. Albert,*[1] *Viviane Ta,*[1]

Gautam Adhikary,[2] *Karine Bourgeois,*[1] *Richard L. Eckert*[2] *and Jeffrey W. Keillor*[1]*

[1] Department of Chemistry and Biomolecular Sciences, University of Ottawa

10 Marie-Curie, Ottawa, Ontario, K1N 6N5 Canada

[2] Department of Biochemistry and Molecular Biology,

University of Maryland School of Medicine, Baltimore, Maryland, USA

ABSTRACT

Human tissue transglutaminase (hTG2) is a multifunctional enzyme. It is primarily known for its calcium-dependent transamidation activity that leads to formation of an isopeptide bond between glutamine and lysine residues found on the surface of proteins, but it is also a GTP binding protein. Overexpression and unregulated hTG2 activity has been associated with numerous human diseases, including cancer stem cell survival and metastatic phenotype. Herein, we present a series of targeted covalent inhibitors (TCIs) based on our previously reported Cbz-Lys scaffold. From this structure-activity relationship (SAR) study, novel irreversible inhibitors were identified that block the transamidation activity of hTG2 and allosterically abolish its GTP binding ability with a high degree of selectivity and efficiency ($k_{inact}/K_I > 10^5$ $M^{-1}min^{-1}$). One optimized inhibitor (**VA4**) was also shown to inhibit epidermal cancer stem cell invasion with an EC_{50} of 3.9 μM, representing a significant improvement over our previously reported 'hit' **NC9**.

INTRODUCTION

Human tissue transglutaminase (hTG2) is a ubiquitously expressed enzyme and is the most studied member of the transglutaminase (TGase) family.[1-2] It is a complex, multifunctional enzyme and the only member of the TGase family that catalyses protein cross-linking and also plays a role in GTP binding and G-protein signalling.[2] Its conformation and consequently its function are tightly regulated by the presence of specific allosteric[3-5] and redox regulators.[5-6] In the extracellular matrix (ECM) and plasma membrane, hTG2 is allosterically modulated by calcium ions[7] and redox proteins to primarily exist in an open or extended conformation that is catalytically active when specific disulfide bonds are reduced.[8] In this conformation the catalytic core, which contains the catalytic triad Cys277, His335 and Asp358, is accessible and capable of catalysing the formation of isopeptide bonds (cross-links) between peptide bound Gln and Lys residues.[9] This cross-linking activity is also referred to as transamidation and occurs via a ping-pong mechanism.[10] First, the nucleophilic active site thiolate (Cys277) attacks an acyl donor substrate (ie. a peptide-bound Gln residue) resulting in the release of one equivalent of ammonia and the formation of the intermediate thioester. Subsequently, the thiolate is regenerated by nucleophilic attack of an acyl acceptor substrate (ie. a peptide-bound Lys residue) to afford the isopeptide product, or the thioester is cleaved by water to afford the deamidated (or hydrolysis) product.[11] Intracellularly, hTG2 is regulated by guanidine-containing nucleotides, such as GTP that bind hTG2 at a site remote from the catalytic active site.[9] Upon GTP binding, hTG2 primarily adopts a closed or compact conformation where the catalytic Cys277 becomes inaccessible. In this closed conformation, it is believed that little or no transamidation activity occurs while several cellular signaling pathways are impacted.[12]

Due to the multifunctional nature and ubiquitous expression of hTG2,[1] it is involved in a variety of normal physiological processes that have been reviewed elsewhere;[2, 13-14] however, its unregulated activity has also been implicated in several disease processes.[15] The unregulated transamidation/deamidation activity of hTG2 has been implicated in atheroscelorsis,[16] pulmonary fibrosis,[17-18] liver fibrosis,[19-20] chronic kidney disease,[21] Alzheimer's disease[22] and celiac disease.[23-26] In addition, recent studies have shown that hTG2 is also an oncogenic protein, where its GTP-binding function has been associated with cancer cell proliferation, metastasis, and cancer stem cell survival.[27-31] Interestingly, hTG2 knockout mice appear developmentally and reproductively normal,[32] mainly displaying delayed wound healing and poor response to stress. Due to the lack of serious and fatal deficiencies observed in hTG2 knockout mice with respect to normal biological functions, as well as its involvement in a wide range of diseases, hTG2 has been proposed as a safe therapeutic target.[32-34]

Several academic and industrial research groups have contributed to the design and evaluation of peptidomimetic and small molecule reversible and covalent hTG2 inhibitors, as summarized in several recent reviews.[35-37] While some studies have focussed on reversible inhibitors of hTG2,[38] the majority have focussed on the development of potent and selective covalent inhibitors that target the nucleophilic active-site Cys277 residue. Some representative examples of peptidic and peptidomimetic irreversible inhibitors of hTG2 are shown in Figure 1. These inhibitors show some structural similarity with respect to the scaffold: a hydrophobic group (Cbz or Ac-Pro) located on the *N*-terminal side of the electrophilic warhead, followed by a small hydrophobic residue *C*-terminal side (Phe or Tyr) or a more extended hydrophobic sequence (e.g. Pro-Phe or Pro-Leu). These structures also display a broad variety of electrophiles used as a warhead, including a sulfonium methyl ketone,[39] a halodihydroisoxazole,[40] a diazomethyl

ketone,[8] an α,β-unsaturated ester[41] and an acrylamide group,[42-47] all of which have been used in the design of hTG2 inhibitors.[35, 37, 48]

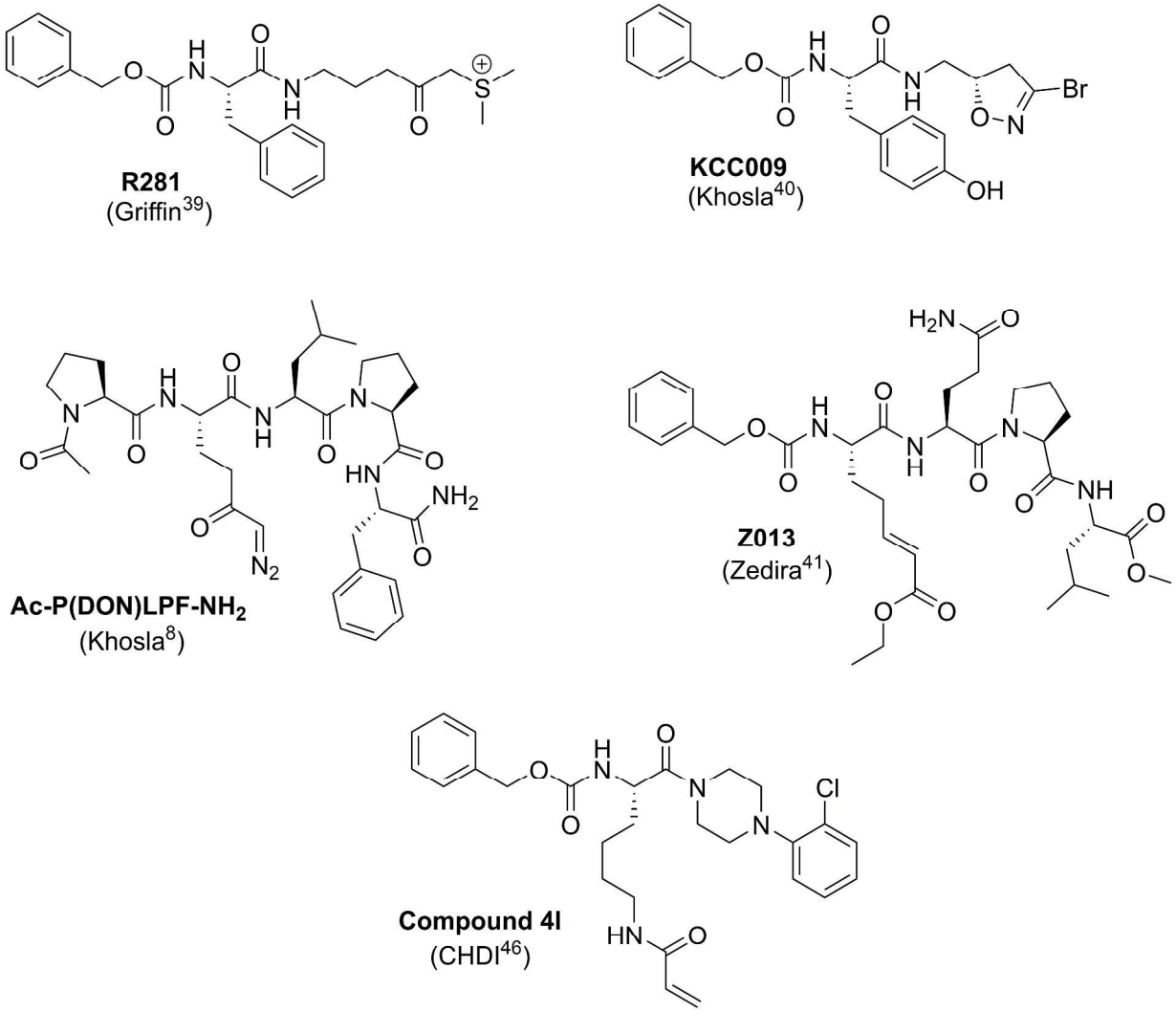

Figure 1. Representative irreversible inhibitors of hTG2 from the recent literature.

The development and use of targeted covalent inhibitors (TCIs) as potential therapeutics has also been reviewed recently.[49] Some of the advantageous features of this class of inhibitors are their high efficiency and extended duration of action. The current consensus of the hTG2 inhibitor field suggests that continued efforts in the design and evaluation of hTG2 inhibitors is needed due to the limited amount of available structural data of the inhibitor-bound protein.[36] In

this work, we present the synthesis and *in vitro* kinetic evaluation of a series of novel irreversible inhibitors that block both the transamidation and GTP-binding activities of hTG2, as well as biological data illustrating cellular efficacy.

RESULTS AND DISCUSSION

Inhibitor Design

Khosla and co-workers have reported[8] a crystal structure of the open form of hTG2 with an irreversible inhibitor bound in the catalytic active site – namely, Ac-P(DON)LPF-NH_2, shown in Figure 1. Based on this crystal structure (PDB code 2Q3Z), the catalytic active site has been described as a relatively hydrophobic binding groove flanking a hydrophobic tunnel that contains the catalytic Cys277 at its base. Previous inhibition studies based on the Cbz-Phe[11, 40, 50] and Cbz-Lys[46, 51] scaffolds have shown that the *N*-terminal Cbz protecting group confers affinity to these irreversible inhibitors (see Figure 1). As such, the Cbz group was maintained throughout this SAR study.

As mentioned above, a variety of electrophilic warheads have also been used in irreversible inhibitors of TGases.[14, 35, 37] We, and others, have found that the acrylamide warhead offers an excellent balance between stability and reactivity for use in targeted-covalent inhibitors of hTG2.[42-47, 50, 52] This balance may also explain why it has seen broad application in TCI's recently developed against other target proteins, as well.[49, 53]

Historically, some of the most potent acrylamide inhibitors that we prepared in previous studies featured a Cbz-Lys scaffold and an acrylamide warhead. For example, we found that compounds **1** and **2** (Figure 2) were remarkably efficient inhibitors of guinea pig liver tissue transglutaminase (gplTG2). Since then, CHDI (Cure for Huntington's Disease Initiative) has reported[46] that our compound **1** (Figure 2) served as a starting point for their SAR study that resulted in **Compound 4l**, shown in Figure 1. In our group, compound **3**, also known as **NC9** (Figure 2) was subsequently designed[51] to be a fluorescent TGase probe.

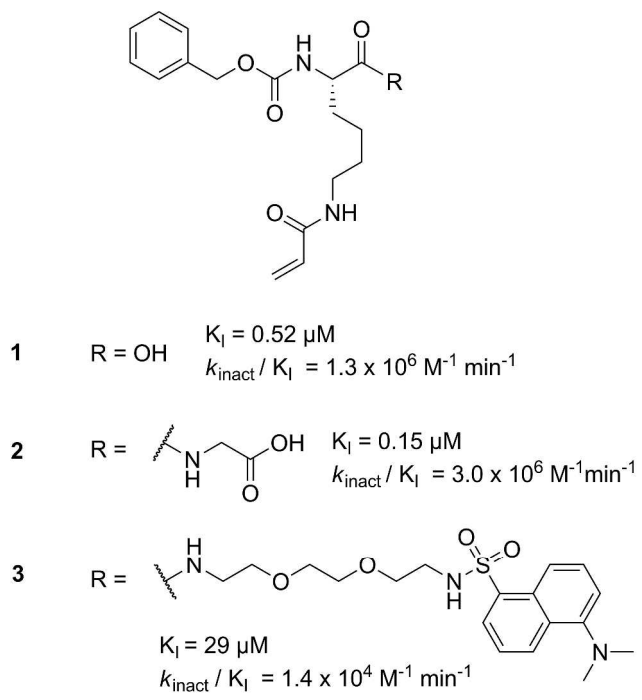

Figure 2. Lysine-based irreversible inhibitors and their kinetic parameters of inhibition against gplTG2.[42, 51]

In this work, we evaluated some of our past compounds such as **1** and **3** against human TG2. We also envisioned a series of modifications that may provide insight into the structural features necessary for potent and selective targeted-covalent inhibition of hTG2. While maintaining the *N*-terminal Cbz protecting group for affinity and the 'select' acrylamide warhead (see above), we systematically varied the length of the side chain, the peptide backbone spacer, and the *C*-terminal R group (Figure 3), seeking to optimize not only inhibition efficiency, but also drug-like properties such as calculated LogP, PSA, and the number of rotatable bonds.

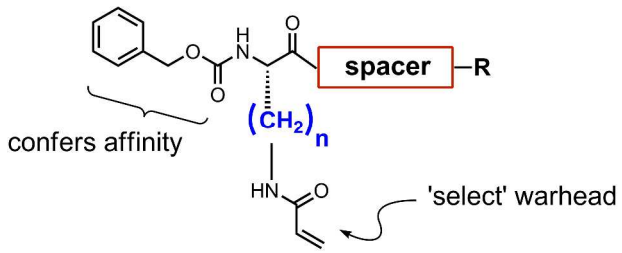

Figure 3. Proposed structural modifications for this SAR study with hTG2.

Synthesis and Structure-Activity Relationship studies

Starting from compound **1**[42, 46] the carboxylic acid group was activated using peptide coupling reagents such as EDC/NHS or EDC/HOBt.[54] From this activated intermediate, a variety of nitrogen nucleophiles were added, giving access to a series of inhibitors in just a few synthetic steps. In the case of compounds **4** and **5** (Scheme 1), ammonium chloride or glycine methyl ester were used as the nucleophile, respectively. From compound **5**, saponification of the methyl ester using LiOH afforded the free carboxylic acid derivative **2**. Collectively, these compounds are abbreviated as Cbz-Lys(Acr)-R deriatives. Irreversible inhibitor **3** was synthesized according to our previously published procedure.[51]

Scheme 1. Synthesis of Cbz-Lys(Acr)-R derivatives of **1**. (a) EDC-HCl, NHS, acetonitrile, rt, 16 h; (b) NH_4Cl, DABCO, acetonitrile, rt, 16 h; (c) glycine methylester, triethylamine, acetonitrile, rt, 4 h; (d) LiOH, THF:H_2O, rt, 1 h.

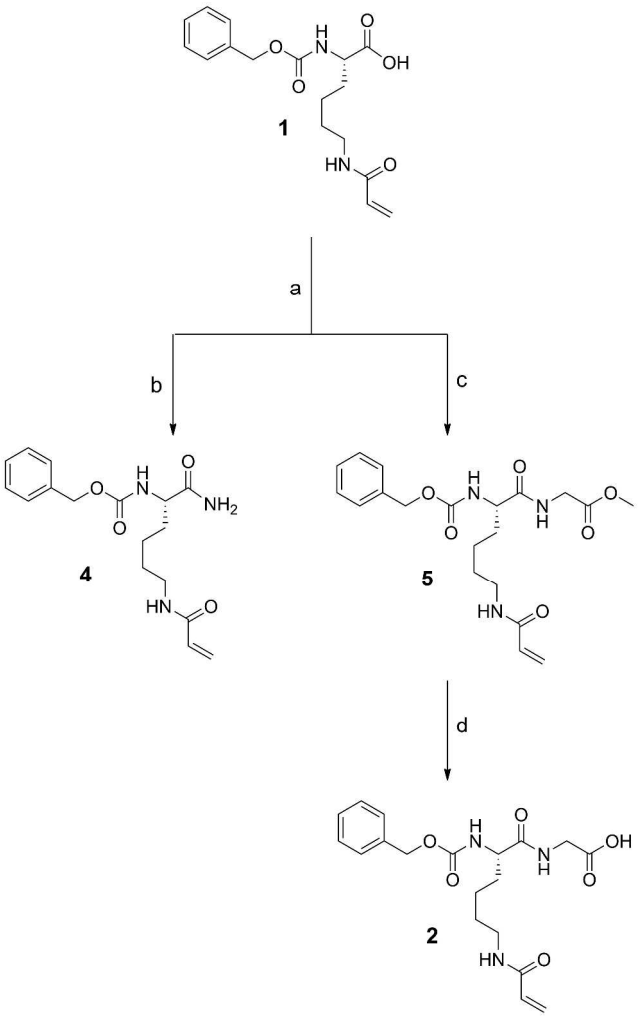

When the carboxylic acid derivatives **1** and **2** were previously synthesized and evaluated as irreversible inhibitors of gplTG2, they displayed excellent kinetic inhibition parameters with K_I values in the high nanomolar range and efficiency constants of 10^6 $M^{-1}min^{-1}$, whereas **3** was two orders of magnitude less efficient.[42, 51] To begin the present SAR study, we re-evaluated

compounds **1**-**2** and **3** as irreversible inhibitors of hTG2. A representative example of this kinetic evaluation is shown in Figure 4.

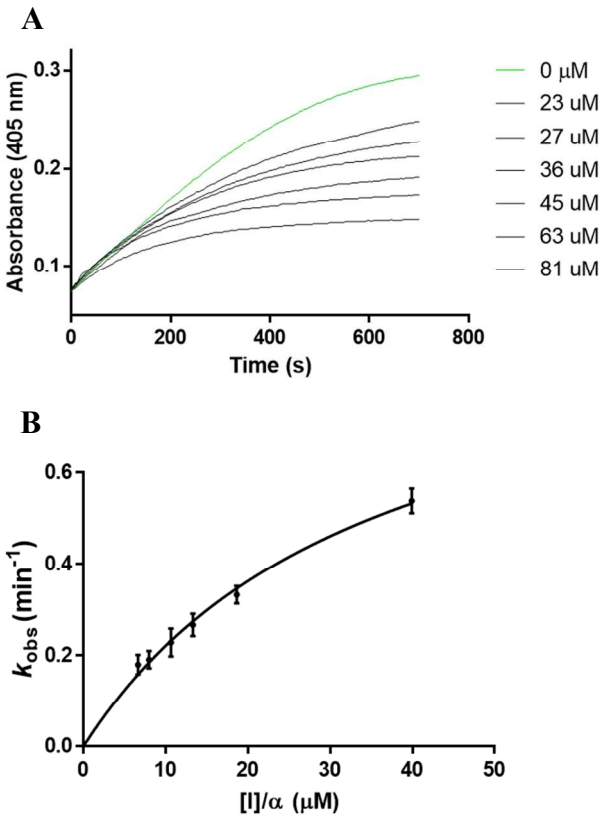

Figure 4. Determination of irreversible inhibition parameters for compound **2** using a previously reported continuous colorimetric assay.[55] (A) Time-dependent inactivation curves of enzymatic reaction in the presence of various concentrations of **2**. (B) Nonlinear regression to a hyperbolic equation of k_{obs} versus varying concentrations of **2**.

Using a colorimetric assay[55] under Kitz & Wilson conditions,[56] rate constants were measured for the time-dependent loss of acyl-transferase activity (Figure 4A). Fitting of the hyperbolic concentration dependence of the observed rate constants of inactivation (Figure 4B) provided the kinetic parameters shown in Table 1 (see Experimental for details).

Table 1. Kinetic parameters of substituted Cbz-Lys(Acr)-R.

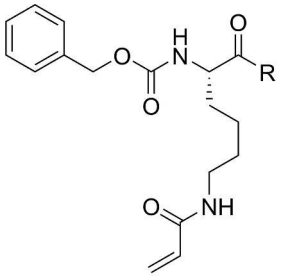

Inhibitor	R group	K_I (μM)	k_{inact} (min^{-1})	k_{inact}/K_I (10^3 M^{-1} min^{-1})
1		60.3 ± 18.6	0.796 ± 0.130	13.2 ± 4.6
2	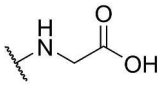	48.1 ± 10.3	1.26 ± 0.17	26.1 ± 6.6
4 [a]		35.1 ± 15.1	1.08 ± 0.46	30.7 ± 2.5
5	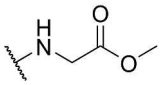	40.0 ± 5.9	1.45 ± 0.12	36.2 ± 6.1
3	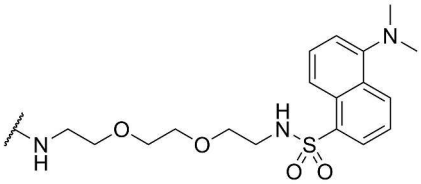	33.9 ± 3.4	2.60 ± 0.17	76.4 ± 9.1

a) Kinetic parameters for compound **4** were determined using a double reciprocal method of data analysis (see Experimental).

While compounds **1** and **2** were among the best irreversible inhibitors of gplTG2, their affinity for hTG2 and their reaction efficiency are shown here to be two orders of magnitude worse. Inhibitor **2**, which contains a glycine linker between the Cbz-Lys(Acr) and the negatively charged carboxylate, shows slightly increased affinity and efficiency compared to **1**. This gain in inhibition efficiency may be due to distancing the negative charge from possible unfavorable interactions in the hydrophobic binding pocket.[8] Replacing the carboxylic acid groups of **1** and **2** with a neutral terminal amide in **4** or a methyl ester in **5** results in minor gains in affinity and efficiency, consistent with the elimination of negative charge and increase in LogP values (3.42 for **4**, 3.09 for **5**). Extending the Cbz-Lys(Acr) scaffold with the addition of a polyethyleneglycol linker and dansyl group in **3** resulted in a comparable inhibition constant to that determined for gplTG2 (K_I = ~30 μM). However, **3** appears to inactivate the human enzyme with a much higher rate constant based on the elevated k_{inact} value of 2.60 min^{-1} compared to 0.483 min^{-1}, for hTG2 and gplTG2 respectively. The observed increase in k_{inact} with respect to hTG2 may be due to a slightly different binding mode that places the acrylamide warhead closer to the active site Cys277 residue. This increased rate constant results in a 5-fold increase in the overall efficiency (k_{inact}/K_I) of **3** as an inhibitor of hTG2.

The results from Table 1 also suggest that the aromatic and hydrophobic dansyl group may provide beneficial contacts with a distal binding pocket of hTG2 that the truncated compounds **1**-**5** cannot access. More specifically, we speculated that the dansyl group of **3** may be discretely bound by hTG2, rather than extended away from it by the PEG spacer, as was our intent in the design of this fluorescent probe.[51] Docking **3** into the open conformation of hTG2 (PDB code 2Q3Z)[8] suggested that the dansyl group may be bound in the hydrophobic pocket on the surface of hTG2 in which the Phe side chain of Ac-P(DON)LPF-NH_2 was bound, in the co-crystal

structure reported by Khosla. In this putative binding model (Figure S1), the PEG spacer forms a long, flexible loop, and few productive interactions with the enzyme.

On the other hand, **3** was tested in biological assays and found to be surprisingly effective against human squamous cell carcinoma. Human TG2 has been shown to be highly elevated in epidermal cancer stem (ECS) cells and hTG2 knockdown or inactivation with 20 μM **3** reduced ECS cell proliferation and survival,[29] the expression of epithelial-mesenchymal transition (EMT) transcription factors and markers,[28] and metastatic phenotype.[28] In TG2 knockout ECS cells, treatment with **3** had no effect, suggesting that its biological activity is not related to off-target interaction.[30] Furthermore, administration of **3** by intraperitoneal injection at 20 mg/kg reduced the growth of mouse xenograft tumors initiated by injection of cancer stem cells.[31] In light of this biological activity, we considered **3** to be an interesting hit, and sought to optimize it further.

For an inhibitor to become a drug candidate, its potency, efficiency and bioavailability must all be optimized. With the ultimate goal of improving all of these features, we considered Lipinksi's[57] and Veber's[58] rules and turned our attention to reducing the number of rotatable bonds and the polar surface area (PSA) in our inhibitors. To this end, we first sought to systematically decrease the length of the diamine spacer between the Cbz-Lys(Acr) and the dansyl functional group of **3**. The mono-dansylated alkyl amines **6-8** in Scheme 2 were synthesized and coupled to the activated carboxylic acid of **1** to give inhibitors **10-12**, and a piperazine linker (**9**) was also coupled to **1** to produce the more rigid inhibitor **13** (also known as **VA4**).

Scheme 2. Synthesis of hTG2 inhibitors with varying spacer length. (a) EDC-HCl, HOBt, triethylamine, acetonitrile, rt, 16 h.

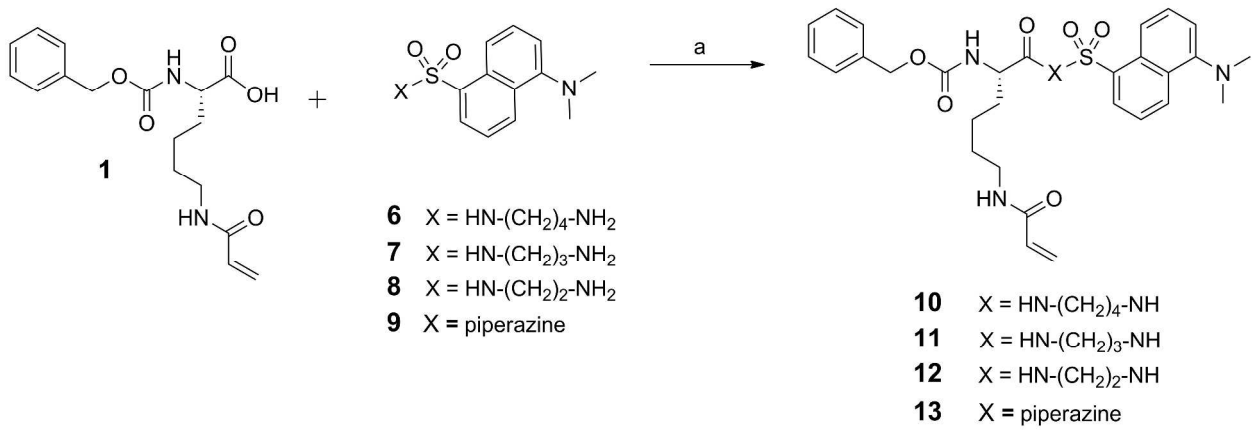

Table 2. Kinetic parameters of irreversible inhibitors with varying backbone spacers.

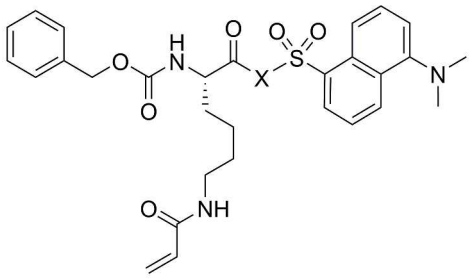

Inhibitor	X group	K_I (μM)	k_{inact} (min^{-1})	k_{inact}/K_I (10^3 M^{-1} min^{-1})	PSA [a] (Å^2)	nRB [a]
3	NH-$(CH_2CH_2O)_2$-CH_2CH_2NH	33.9 ± 3.4	2.60 ± 0.17	76.4 ± 9.1	164	23
10 [b]	HN-$(CH_2)_4$-NH	27.1 ± 11.9	2.19 ± 0.94	80.8 ± 4.7	146	19
11 [b]	HN-$(CH_2)_3$-NH	30.5 ± 9.4	0.85 ± 0.25	27.6 ± 1.7	146	18
12 [b]	HN-$(CH_2)_2$-NH	23.5 ± 3.1	1.45 ± 0.12	61.5 ± 9.6	146	17
13	piperazine	12.9 ± 2.6	1.40 ± 0.13	107 ± 23.8	128	14

a) Polar Surface Area and the number of Rotatable Bonds were calculated using the Molinspiration molecular property calculation engine (http://www.molinspiration.com).

b) Kinetic parameters for compounds **10-12** were determined using a double reciprocal method of data analysis (see Experimental).

As shown in Table 2, reducing the spacer length from eight atoms in **3** to four atoms in compound **10** resulted in a dramatic reduction in the number of rotatable bonds and PSA, but little change with respect to the kinetic parameters measured. Interestingly, reducing the spacer

to three methylene groups (**11**) resulted in a marked reduction in efficiency, mainly due to a significant drop in the inactivation rate constant. Decreasing the spacer length to two methylene units (**12**) restored inhibitor efficiency to the values seen for the hit compound **3**. Maintaining the distance associated with a two-methylene spacer but in the form of the more rigid piperazine group gave inhibitor **13**, displaying the best inhibition parameters in the series. In addition to exceeding the overall inhibition efficiency of **3**, inhibitor **13** also showed a greater than two-fold reduction in the inhibition binding constant, suggestive of more favorable interactions with the binding pocket of hTG2 compared to inhibitors with more flexible spacers. It is interesting to note that CHDI also discovered the suitability of the piperazine group at this position in analogous inhibitors, but from an expansion strategy among a series of *C*-terminal tertiary amides.[46] With a PSA below 140 $Å^2$ and nearly half as many rotatable bonds as **3**, we were also hopeful that the bioavailability of **13** would be substantially improved (see below).

Using **13** as a new parent compound, additional inhibitors were then prepared that contained the dansyl piperazine but whose side chains bearing the acrylamide warhead were systematically varied with respect to their length. Compounds **14–16** were synthesized from commercially available starting materials using modified literature procedures,[43, 46] and were coupled to the mono-dansyl piperazine to afford irreversible inhibitors **17-19** (Scheme 3).

Scheme 3. Synthesis of irreversible hTG2 inhibitors **17-19.** (a) EDC-HCl, HOBt, triethylamine, acetonitrile, rt, 16 h.

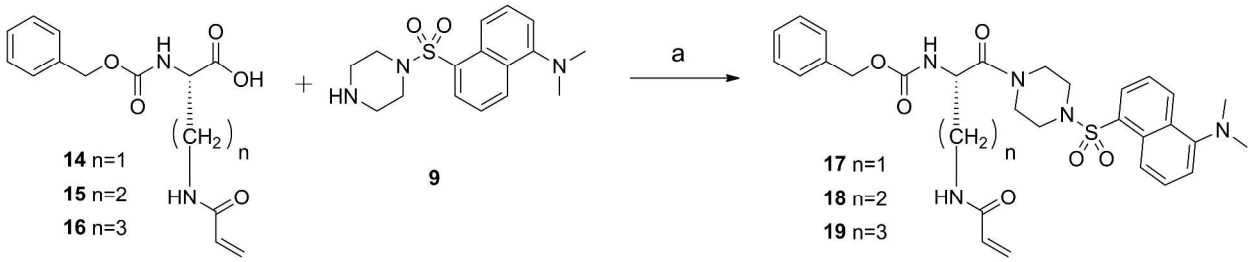

Table 3. Kinetic parameters of derivatives having varied side chain length.

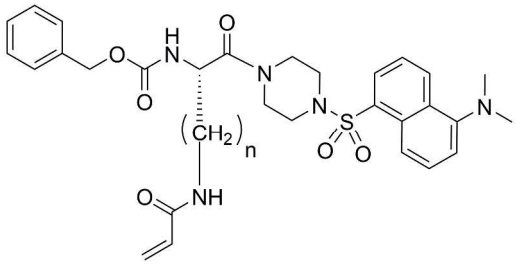

Compound	$(CH_2)_n$	K_I (μM)	k_{inact} (min^{-1})	k_{inact}/K_I (10^3 M^{-1} min^{-1})	nRB [a]
17	n = 1	n.d.	n.d.	n.d.	11
18	n = 2	n.d.	n.d.	n.d.	12
19 [b]	n = 3	47.7 ± 37.8	1.18 ± 0.93	24.7 ± 2.2	13
13	n = 4	12.9 ± 2.6	1.40 ± 0.13	107 ± 23.8	14

a) The number of Rotatable Bonds was calculated using the Molinspiration molecular property calculation engine (http://www.molinspiration.com).

b) Kinetic parameters for compound **19** were determined using a double reciprocal method of data analysis (see Experimental). n.d = not detectable

As shown in Table 3, although reducing the length of the side chain reduced the number of rotatable bonds in inhibitors **17-19**, it also had a drastic effect on the efficacy of the inhibitors. Time-dependent inhibition of hTG2 within a reasonable inhibitor concentration range was only observed for compound **19** and consequently we were unable to determine the kinetic parameters for **17** and **18**. As another means of comparison, we tested high concentrations of inhibitors **17-19** in our colorimetric assay and measured relative observed rate constants (k_{obs}) from the time-dependent inactivation curves, as shown in Figure 5.

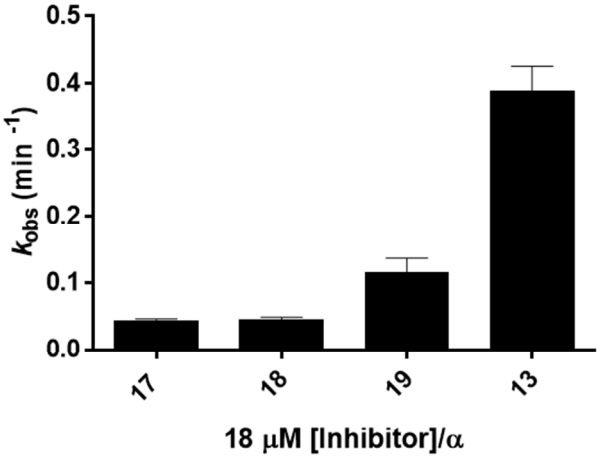

Figure 5. Observed rate constants (k_{obs}) of inactivation of hTG2 with 18 μM of inhibitors **17-19**.

From both Table 3 and Figure 5, it is obvious that reducing the number of methylene units of the side chain below 4 results in a dramatic loss of activity. These results are consistent with previous studies performed on the Cbz-Phe-X and Cbz-X-Gly scaffolds.[42] We hypothesize that both the Cbz and dansyl functional groups present favorable contacts with the extended hydrophobic binding pocket on the surface of hTG2[8] and thus help to position the acrylamide warhead for attack by Cys277 at the base of the active site tunnel. A sidechain of one or two

methylene units is apparently not long enough to position the acrylamide group for nucleophilic attack, and therefore no significant enzyme inactivation is observed. Extending the side chain to three methylene units results in the reappearance of activity for inhibitor **19**, but only modestly in comparison to **3** and **13**. It is evident that the side chain length is a critical component of this inhibitor scaffold for successful inhibition of hTG2.

Having established the advantages of a piperazine linker and a four-methylene side chain, we moved our attention to modification of the dansyl group. We began by synthesizing derivatives that maintained the sulfonamide connection, while replacing the dansyl group with various aromatic and aliphatic functional groups. Our goal was to probe the interaction with the putative hydrophobic binding pocket, while optimizing for the number of rotatable bonds and lipophilicity. First, the piperazine sulfonamide intermediates **21** – **29** were synthesized (see supporting information), followed by peptide coupling with carboxylic acid **1** to give final compounds **30** – **38** (Scheme 4).

Scheme 4. Synthesis of sulfonamide-containing hTG2 inhibitors. (a) triethylamine, DCM, rt, 16 h; (b) EDC-HCl, HOBt, triethylamine, acetonitrile, 16 h.

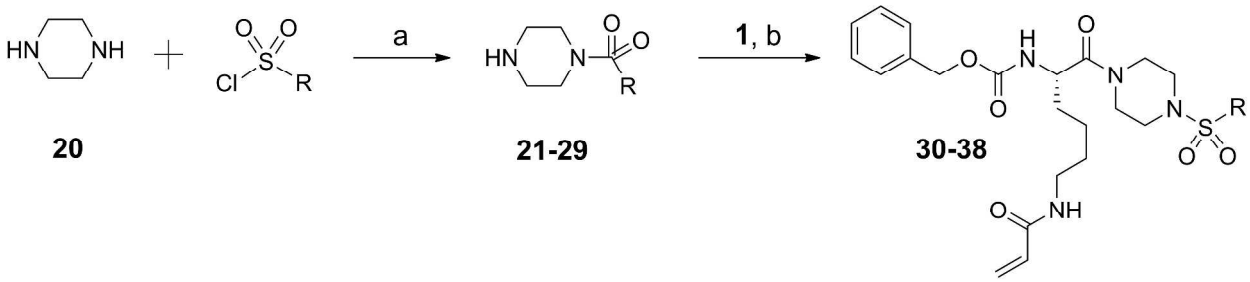

Compound **30** differs from **13** only by the lack of the dimethyl amino group on the naphthalene ring, so these inhibitors are very similar with respect to calculated LogP and rotatable bonds. Interestingly, the inhibition constants (K_I) for both **30** and **13** are also very comparable (Table 4); however, the rate constant of inactivation (k_{inact}) of **30** is more than three-fold less than that of **13**, resulting in a lower overall inhibition efficiency for **30**. Changing the orientation of the naphthyl moiety in compound **31** gave a modest gain in inhibition efficiency. Reducing the size of the aromatic ring from naphthyl to phenyl in compound **32** resulted in a slight decrease in the calculated LogP, to below 5, although its inhibition kinetics were no better than those of **31**. The introduction of the more flexible phenylacetyl group in compound **33** resulted in a reduction of inhibition efficiency to values comparable with **30**. Comparison of the kinetic data for compounds **30** – **33** suggests that the binding pocket is relatively indiscriminate and will accept moderate to large hydrophobic groups, and that there is little difference in the calculated LogP values, as expected.

The importance of the aromaticity of these substituents was then investigated by synthesizing and evaluating non-aromatic compounds **34** – **37**. Based on the kinetic data shown in Table 4, aromaticity is not necessary to achieve modest inhibition efficiency; the cyclohexyl (**34**), isopropyl (**35**), ethyl (**36**) and methyl (**37**) sulfonamides all gave comparable inhibition values to

those of the aromatic derivatives. Interestingly, the electron-rich thiophene sulfonamide derivative (**38**) showed poor inhibition, while the methyl sulfonamide (**37**) had the best inhibition kinetics of the series. Furthermore, inhibitor **37** has a significantly lower calculated LogP value, fewer rotatable bonds and a molecular weight below of only 480.6 g/mol, all of which may slightly favor its cellular permeability.

Table 4. Kinetic parameters of piperazine sulfonamide derivatives.

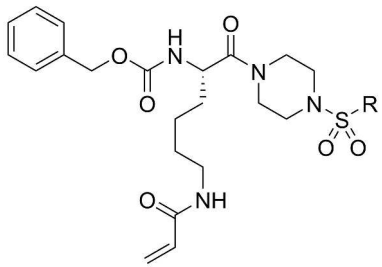

Inhibitor	R group	K_I (μM)	k_{inact} (min^{-1})	k_{inact}/K_I (10^3 M^{-1} min^{-1})	LogP [a]	PSA [a] (Å^2)	nRB [a]
13	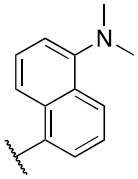	12.9 ± 2.6	1.40 ± 0.13	107 ± 23.8	5.49	128	14
30	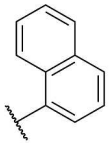	10.4 ± 1.8	0.39 ± 0.03	37.2 ± 7.1	5.43	125	13
31	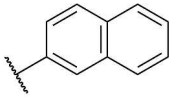	6.7 ± 1.1	0.38 ± 0.03	57.3 ± 10.6	5.46	125	13

32	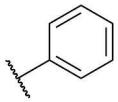	8.8 ± 1.5	0.47 ± 0.04	53.3 ± 9.8	4.28	125	13
33	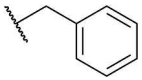	14.7 ± 3.2	0.47 ± 0.06	34.9 ± 8.7	4.34	125	14
34	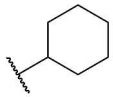	11.0 ± 1.1	0.69 ± 0.03	62.9 ± 7.1	4.65	125	13
35		9.1 ± 1.6	0.50 ± 0.03	54.7 ± 10.4	3.48	125	13
36		36.0 ± 3.6	1.42 ± 0.09	39.4 ± 4.5	3.12	125	13
37		6.4 ± 1.8	0.50 ± 0.05	78.4 ± 23.7	2.74	125	12
38	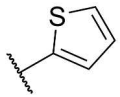	40.1 ± 6.0	1.48 ± 0.13	36.8 ± 6.4	4.22	125	13

a) LogP and the number of Rotatable Bonds were calculated using the Molinspiration molecular property calculation engine (http://www.molinspiration.com).

The final series of derivatives that were investigated was also constructed from a Cbz-Lys(Acr)-pip-X scaffold, but the *C*-terminal sulfonamide group was replaced with a carboxamide functional group. This was expected to decrease the polar surface area of the inhibitors, and possibly to orient the *C*-terminal hydrophobic group slightly differently, due to the conformational difference between a carboxamide and a sulfonamide. Piperazine amide intermediates **40** – **48** were prepared from the Boc-protected piperazine (**39**). Various acid chlorides or activated carboxylic acids were also coupled to **39** to afford the desired Boc-piperazine intermediates. Removal of the Boc group, followed by peptide coupling with acrylamide **1** gave the desired final compounds **49** – **57** (Scheme 5).

Scheme 5. Synthesis of carboxamide hTG2 inhibitors. (a) EDC-HCl, NHS, acetonitrile, rt, 16 h; (b) triethylamine, acetonitrile, rt, 4 h; (c) triethylamine, DCM, rt, 4 h.

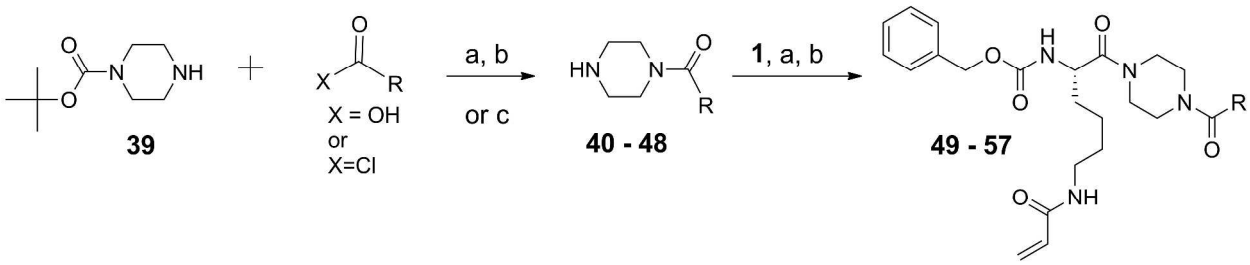

Table 5. Kinetic parameters of piperazine amide derivatives.

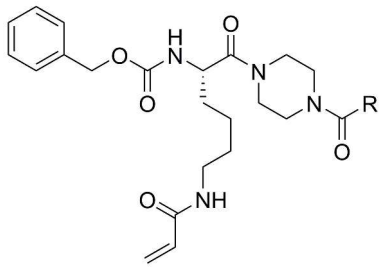

Inhibitor	R group	K_I (μM)	k_{inact} (min^{-1})	k_{inact}/K_I (10^3 M^{-1} min^{-1})	LogP [a]	PSA [a] (Å^2)	nRB [a]
49 (AA9)	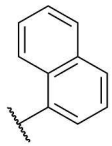	8.9 ± 1.0	0.90 ± 0.05	101 ± 12.8	5.09	108	12
50 (AA10)	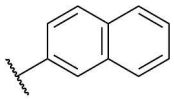	13.4 ± 2.3	1.21 ± 0.13	90.3 ± 18.0	5.11	108	12
51	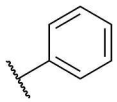	36.6 ± 4.8	4.77 ± 0.46	130 ± 21.2	3.93	108	12
52	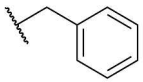	20.0 ± 5.8	2.26 ± 0.37	113 ± 37.5	4.49	108	13

53		52.1 ± 6.7	2.06 ± 0.18	36.9 ± 6.1	2.73	108	11
54	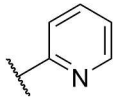	32.1 ± 5.4	2.93 ± 0.29	91.3 ± 17.9	3.23	121	12
55	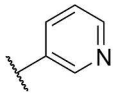	23.4 ± 2.2	1.44 ± 0.07	61.4 ± 6.4	2.69	121	12
56	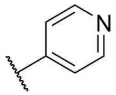	38.7 ± 5.7	1.43 ± 0.13	37.0 ± 6.4	2.64	121	12
57 (VA5)	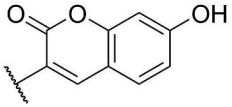	11.2 ± 2.6	0.69 ± 0.09	62.1 ± 16.4	3.43	158	12

a) LogP, Polar Surface Area and the number of Rotatable Bonds were calculated using the Molinspiration molecular property calculation engine (http://www.molinspiration.com).

Direct comparison of the 1-naphthyl (**49**), 2-naphthyl (**50**),[59] phenyl (**51**) and benzyl (**52**) amide derivatives in Table 5 to their corresponding sulfonamide derivatives in Table 4 suggests that the presence of an amide functional group in lieu of the sulfonamide is beneficial for the inhibition of hTG2. All four of these aromatic derivatives (**49** – **52**) show at least a two-fold increase in overall inhibition efficiency compared to their sulfonamide counterparts (**30** – **33**), and a significant reduction in their polar surface areas. Surprisingly, this trend does not hold for the acetyl derivative (**53**). Although the polar surface area is less than that of the methyl sulfonamide derivative (**37**), as expected, its overall inhibition efficiency almost three times lower.

The introduction of an *N*-heterocycle in the form of three different pyridine isomers showed an interesting trend in inhibition efficiencies as the nitrogen was moved around the aromatic ring relative to the amide bond (Table 5). The picolinamide derivative (**54**) showed the best overall efficiency, followed by the nicotinamide derivative (**55**) and then the isonicotinamide derivative (**56**). While all three of the *N*-heterocycle inhibitors had lower calculated LogP values compared to the non-polar phenyl compound (**51**), they were also significantly less efficient inhibitors. This may suggest that a heterocycle substituent is not necessary but can be tolerated by hTG2; perhaps conformational rotation of the pyridine ring allows the polar nitrogen of the picolinamide derivative to be oriented towards solvent, while the rest of the ring occupies a hydrophobic cavity. Finally, the coumarin derivative (**57,** aka **VA5**)[30, 59-60] was intended for use as a cellular fluorescent probe that would be visible in the blue region. We were gratified to note that the inhibition kinetic parameters of this compound were comparable to those of **13**, although its polar surface area was considerably larger, raising concerns over its permeability.

Overall, upon consideration of affinity, efficiency, and physicochemical properties, we judged **13** and compound **49**, also known as **AA9**, to be the best lead compounds from the sulfonamide and amide piperazinyl linked derivatives. Both compounds are highly efficient irreversible inhibitors ($k_{inact}/K_I > 10^5$ $M^{-1}min^{-1}$) and have polar surface areas smaller than 140 $Å^2$; however, both have calculated LogP values just over 5, and more than 10 rotatable bonds.

Inhibition of GTP-binding

As mentioned above, unregulated transglutaminase activity has been implicated in the pathogenesis of several diseases. In most of these diseases, it is the enzymatic transamidase function of hTG2 that is believed to contribute to the pathology; however, more recently it has been shown that the GTP-binding ability of the enzyme is involved in certain types of cancer.[2, 27-28] Consequently, targeting hTG2 to abolish its enzymatic activity and/or GTP binding offers a potential therapeutic approach towards treatment of associated diseases.

A crystal structure of hTG2 in complex with GDP illustrated how guanidine nucleotide binding causes the two *C*-terminal β-barrel domains to be folded over the catalytic core,[9] showing how acyl-transfer activity and GTP-binding are conformationally mutually exclusive. Our irreversible inhibitors are competitive with respect to the acyl-donor substrate of hTG2, and we have observed by mass spectrometry that one equivalent of **3**, **50**, or **57** are covalently incorporated into irreversibly inhibited hTG2,[59] presumably through reaction with the active site cysteine. Therefore, our inhibitors should not compete directly with GTP binding. However, we have also shown, by both FRET-FLIM[12, 30] and by CE-MS,[59, 61] that micromolar concentrations of these acrylamide-based irreversible inhibitors can lock hTG2 in its open/extended conformation, rendering hTG2 incapable of binding GTP. To that end, two of our lead

compounds (**13** and **49)** were tested further for their ability to abolish GTP binding. In this work, GTP binding was assessed using a fluorescent non-hydrolysable GTP analogue (GTPγS FL BODIPY) whose fluorescence increases when bound to a GTP-binding protein.[30, 62] According to this evaluation, hTG2 showed significant loss in GTP binding ability after incubation with our inhibitors (Figure 6). Therefore, in addition to their confirmed ability to irreversibly inactivate TGase transamidation function (see Experimental), presumably by covalently modifying the active site Cys277 residue, **13** and **49** are also clearly capable of abolishing GTP binding nearly completely.

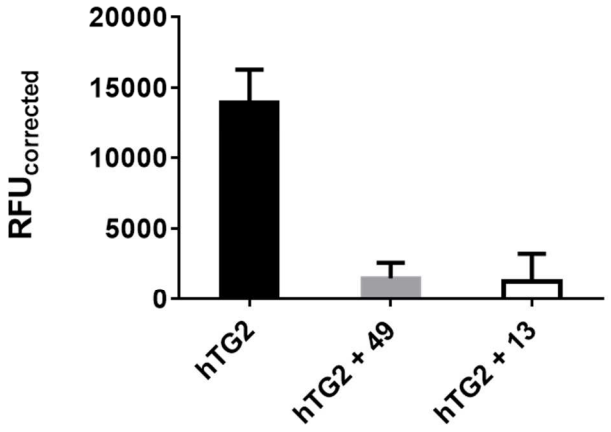

Figure 6. Suppression of GTP binding activity using 3 μM of GTP-γ-S FL BODIPY after inhibition of hTG2 with **13** and **49**.

To gain more insight into the structural requirements for inhibition of GTP binding, we tested an inhibitor lacking two key structural components: namely the *C*-terminal functional group and the piperazine linker. Even without these structural features, compound **4** was still an efficient irreversible inhibitor of hTG2's catalytic activity, as shown in Table 1, and it was also able to

abolish GTP binding (Figure S2). However, using iodoacetamide (see Figure 7), a non-selective irreversible inhibitor of many acyltransferases,[7] also resulted in the irreversible inhibition of hTG2 acyltransferase activity, but did not perturb its GTP-binding ability (Figure S3). This suggests that the covalent addition of the acetamide group does not prevent the enzyme from adopting its closed conformation. By extension, other small irreversible inhibitors such as **L682777**[63-64] and **R283** [65] (the correct structures of which are shown in Figure 7), both of which add an acetone moiety to the active site nucleophile, are also unlikely to affect GTP binding. In the future, systematic structural modification of our irreversible inhibitors may lead to the development of minimalist inhibitors that can irreversibly inhibit TGase activity with a degree of selectivity, without perturbing GTP binding. But at the present time, it is noteworthy that we have provided unambiguous biochemical evidence that our inhibitors abolish both acyl transferase and GTP-binding activities *in vitro*. As discussed above, we have shown previously that our inhibitors stoichiometrically and covalently modify hTG2,[59] presumably through their reaction with the active site Cys277. We have also shown previously that this reaction locks hTG2 in an open conformation.[12, 30, 59, 61] Taken together, this represents a novel allosteric mechanism for inhibiting GTP binding, without the use of GTP analogues, an approach that may suffer from the lack of selectivity.

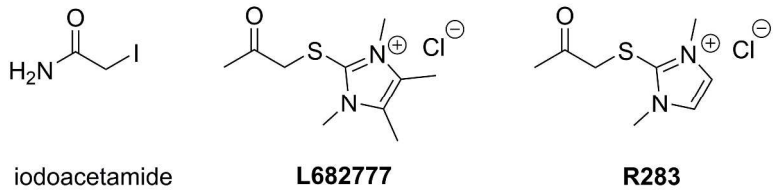

Figure 7. Small irreversible TGase inhibitors.[64-66]

Isozyme selectivity

We next assessed the selectivity of our most studied inhibitors, **13** and **3**, for their reaction with hTG2 over other members of the TGase family. These two efficient irreversible inhibitors were tested against four therapeutically relevant isoforms of human transglutaminase: FXIIIa, hTG3, hTG1 and hTG6. We found that our previously reported continuous colorimetric assay,[55] using Cbz-Glu(γ-p-nitrophenyl ester)Gly as a substrate, was capable of effectively reporting the activity of hTG1 and hTG6 (Figures S4-S5). As for the other TGases, FXIIIa and hTG3, a commercially available continuous fluorescent assay that utilizes a peptidic FRET-quenched substrate was used.[66-67] The rate constant of enzyme inactivation (k_{obs}) for a specific concentration of inhibitor was obtained using Kitz and Wilson conditions[56] (Figures S7-S10). Inhibitor concentrations were adjusted to account for competition with substrates in each enzymatic reaction. In general, our potent irreversible inhibitors showed excellent selectivity towards hTG2 over the other isozymes (Table 6). Both **13** and **3** demonstrated superior selectivity towards hTG2 over hTG3a by about 390-fold. **13** was 48-fold less reactive with hTG1, 80-fold less reactive with FXIIIa and no inhibition was observed with hTG6 compared to inhibition of hTG2. In addition, **13** illustrated a lower reactivity towards other TGase isozymes compared to **3**. The subsequent *in vitro* selectivity over homologous TGases bodes well for *in vivo* selectivity.

Table 6. Selectivity of **13** and **3** against TGase isoforms.

Compound #	k_{obs} (10^{-3} min $^{-1}$)				
	TG2	**TG1**	**TG3a**	**TG6**	**FXIIIa**
3	390 ± 49	78.9 ± 5.9	1.01 ± 0.09	6.16 ± 0.14	5.91 ± 1.59
13	394 ± 37	8.27 ± 0.76	0.65 ± 0.21	n.d.	4.08 ± 0.77

n.d = inhibition not detected

Kinetic comparisons

In the context of previous work in the field, we wanted to benchmark our inhibitors against some of those known in the literature. For example, CHDI has reported extensive SAR studies [44-46] of many novel TCIs of hTG2, including those incorporating a similar Cbz-Lys scaffold, based on our original inhibitor **1**.[42-43] We chose two compounds from their work, inhibitor **58** (Figures 1 and 8), the best inhibitor reported,[46] and inhibitor **59** (Figure 8). The potency of these inhibitors was reported in the form of IC_{50} values (62 nM for **58** and 730 nM for **59**).[46]

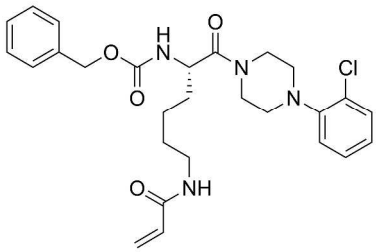

58

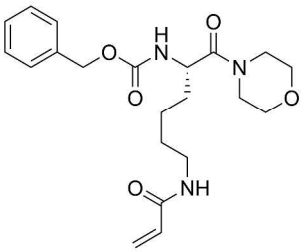

59

Figure 8. Targeted-covalent inhibitors reported by CHDI.[46]

For reversible inhibitors, IC_{50} values are highly relative, and depend upon the assay used to measure activity, the concentration of substrate used and the mode of inhibition, to name a few factors.[14] But for irreversible inhibition, IC_{50} values are even less meaningful, if not inappropriate, since inhibitor activity will also depend on the time of incubation in different ways for different inhibitors.[68] For these reasons, we chose to re-evaluate inhibitors **58** and **59** using the same assay applied to our novel inhibitors. This evaluation gave inhibition parameters of k_{inact} = 0.974 min^{-1}, K_I = 17.4 μM, k_{inact}/K_I = 56.0 × 10^3 M^{-1} min^{-1} for **58** and k_{inact} = 1.47 min^{-1}, K_I = 28.9 μM, k_{inact}/K_I = 51.0 × 10^3 M^{-1} min^{-1} for **59**. We were pleased to note that compared to some of the most potent TCIs reported for hTG2 (i.e. **58** and **59**), our best inhibitors (**13** and **49**) are nearly twice as efficient, chiefly due to their higher affinity.

Cellular evaluation

Over the course of this SAR study, optimization from **3** to **13** was based on both the *in vitro* efficiency of the TCI, and on physicochemical properties that may correlate with cellular permeability.[57-58] In particular, the PSA of **13** is substantially lower than that of **3** (and below 140 $Å^2$)[58] and **13** has significantly fewer rotatable bonds (see Tables 2 and 4). Both of these compounds were therefore evaluated in a cellular assay to see if this optimization correlated with improved biological activity.

An enhanced ability to invade matrigel (collagen) is a property of tumor-initiating cells that is associated with cancer metastasis. It has been shown previously that epidermal cancer stem (ECS) cells invade efficiently and migrate rapidly, relative to non-stem cancer cells and that these properties are associated with enhanced tumor formation.[69] We have also shown that 20 μM of **3** is sufficient to reduce ECS migration by nearly 50% relative to vehicle-treated cells.[28]

To determine the *relative* potency of **3** and **13**, we monitored the ability of ECS cells to migrate through matrigel treated with either of these inhibitors over a concentration range of 1-50 μM. As can be seen in the dose-response data shown in Figure 9, both inhibitors are capable of inhibiting ECS cell migration. The migration data for **13** could be fitted to provide an EC_{50} value of 3.9 μM (see Experimental). However, the data for **3** could not be fitted accordingly and can only be estimated to be >20 μM, in rough agreement to what was previously reported.[28] The superior potency of **13** compared to **3** in this cellular assay validates the optimization of *in vitro* efficiency and physicochemical properties of this SAR study.

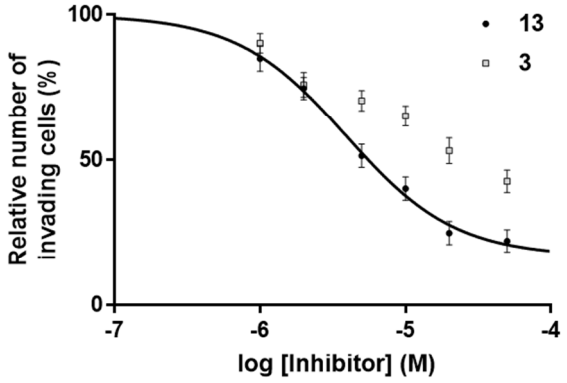

Figure 9. Dose-response data for inhibition of ECS invasion by **13** and **3**. The solid line was fitted through the data for **13**, providing an EC_{50} value of 3.9 μM (see Experimental).

CONCLUSIONS

We have prepared and evaluated a series of novel irreversible inhibitors of hTG2, based on our previously validated[42] Cbz-Lys scaffold and bearing an acrylamide warhead. From an SAR study that considered affinity, efficiency and physicochemical properties, **13** and **49** were judged to be the best lead compounds among the sulfonamide and piperazinyl amide derivatives. We also examined the ability of select inhibitors to disrupt the GTP-binding activity of hTG2. Both **13** and **49** were shown to abolish GTP binding. Considering the known effects of our inhibitors on hTG2 conformation,[59] we surmise that this conformational modulation of the enzyme to its open/extended form results in disruption of the GTP binding pocket. Furthermore, both our 'hit' **3** and the optimized **13** demonstrate excellent selectivity over homologous TGase isoforms.

Compound **3** has also been used previously to define the pathogenic role of hTG2 in human squamous cell carcinoma. Human TG2 has been shown to be highly elevated in ECS cells and hTG2 knockdown or inactivation with **3** reduced ECS cell survival.[29] Knockdown of hTG2, or inhibition with **3**, resulted in a reduced expression of epithelial-mesenchymal transition (EMT) markers, and reduced metastatic phenotype.[28] Additional evidence also suggests that it is the GTP binding ability of hTG2 that enhances cancer cell and cancer stem cell survival,[28, 31] and that **3** and **13** are able to inhibit both the transamidation and GTP binding activity of hTG2 in a cellular context.[30] Herein, we show that the optimized **13** is roughly an order of magnitude more potent than **3** in a cellular assay, presumably due to its enhanced efficiency and physicochemical properties.[58] Given the potent and selective nature of our lead inhibitors demonstrated herein, we believe they show promise for targeting hTG2 in anti-cancer stem cell therapy.

EXPERIMENTAL SECTION

In Vitro Assays.

Colorimetric transamidase activity assay. The activities of hTG1, hTG2 and hTG6 were measured via a colorimetric assay using the chromogenic substrate Cbz-Glu(γ-*p*-nitrophenyl ester)Gly (**AL5**).[55] The assay was conducted at 25 °C in 100 mM MOPS buffer (pH 6.5) containing 3.0 mM $CaCl_2$ and 50 μM EDTA. Enzymatic inhibition assays were run under Kitz & Wilson conditions[56] established for each transglutaminase isoform by varying the concentration of substrate to be 112 μM, 112 μM, and 436 μM of **AL5** for hTG1, hTG2, and hTG6, respectively. A stock solution of **AL5** was prepared in DMSO such that the final concentration of this co-solvent was constant at 2.5 % v/v. Stock solutions of the inhibitors were made in the buffer system previously described. The reaction was initiated with the addition of 40-60 mU/mL of the respective enzyme (0.10 μM hTG1, 0.25 μM hTG2 or 0.32 μM hTG6). Product formation was monitored at 405 nm in a polystyrene 96-well microplate using a BioTek Synergy 4 plate reader. Mono-exponential time-dependent inactivation was observed for all the inhibitors studied. Observed first-order rate constants of inactivation (k_{obs}) were determined from non-linear regression fit to a mono-exponential model (Equation 1) of the observed absorbance of the enzymatic hydrolysis product, *p*-nitrophenolate (pNP). These rate constants (k_{obs}) were in turn fit to a saturation kinetics model (Equation 2), by non-linear regression, providing the kinetic parameters k_{inact} and K_I, as previously described by Stone and Hofsteenge.[70] A double reciprocal plot of equation 2 was applied when the observed rate constant of inactivation (k_{obs}) did not demonstrate saturation at high inhibitor concentrations, or when solubility issues were encountered. Experiments were done in triplicate and variation between repeats was less than 30 %.

$$f(pNP) = [pNP]_0 + \left(\text{Plateau-}\ [pNP]_0\right)(1 - e^{(k_{obs}t)}) \qquad \textbf{(1)}$$

$$k_{obs} = \frac{k_{inact}[I]}{[I] + K_I\left(1 + \frac{[S]}{K_M}\right)} \qquad \textbf{(2)}$$

Inhibition irreversibility. Compound **13** was incubated with hTG2 and the reaction solution was filtered over a 10-kDa molecular weight cut-off membrane, after which the residual enzyme solution was diluted and subjected to an activity assay as described previously. In comparison to a positive control of uninhibited hTG2, the inhibited enzyme exhibited no recovered activity (data not shown). Furthermore, we have previously demonstrated by mass spectrometry that incubation with acrylamide inhibitor **13** results in the incorporation of one equivalent of inhibitor.[59]

Fluorescence isopeptidase activity assay. The isopeptidase activity of pre-activated TG3a and FXIIIa (purchased from Zedira) was measured via a fluorescence-based assay[67] using the commercially available peptidic FRET quenched probe **A101** from Zedira. Briefly, the final concentration in the reaction mixture contained 50 mM Tris (pH 7.0), 10 mM $CaCl_2$, 100 mM NaCl, 2.8 mM TCEP, 50 μM **A101** and 14 mM H-Gly-OMe. The reaction was monitored at 25 ˚C using a BioTek Synergy 4 plate reader (Ex/Em: 318/413 nm). Enzymatic inhibition assays were run under Kitz and Wilson conditions,[56] which was established for TG3a and FXIIa at a substrate (**A101**) concentration of 50 μM using enzyme concentrations of 0.17 μM and 0.11 μM for TG3a and FXIIIa, respectively.

In vitro GTP binding assay. GTP binding was measured using a method similar to that reported previously.[62] For all experiments, GTP binding was measured using 3 μM of the fluorescent,

non-hydrolysable GTP analogue BODIPY GTP-γ-S (Invitrogen), whose fluorescence increases when bound by protein. hTG2 (8-10 μg) was incubated at 25 ºC for 30 minutes with or without irreversible inhibitor (2 x K_I) with 3.0 mM $CaCl_2$ in 100 mM MOPS (pH = 6.54). The buffer was then exchanged to 100 mM MOPS (pH = 7.0), 1 mM EGTA and 5 mM $MgCl_2$ to remove calcium using a 10-kDa molecular weight cut off membrane. The fluorescent GTP analog was then added to give a final concentration of 3.0 μM and fluorescence was then measured on a microplate reader after 10 minutes of incubation (Ex/Em: 490/520 nm).

Cell invasion assay

To measure cell invasion, matrigel (Corning, cat # 354234) was diluted to 250 μg/mL and 120 μL was added to the upper chamber of Transwell Chambers (Corning, #353097, 1-cm diameter, 8-μm pore size) and allowed to solidify. SCC-13 monolayer cells were suspended in spheroid medium[31, 71] containing 1% fetal calf serum and 20,000 cells were plated into each upper chamber atop the matrigel. The bottom chamber contained spheroid medium supplemented with 10% FCS and the appropriate concentration (1-50 μM) of either **3** or **13**. After an 18-h incubation in a 37 ºC incubator, cells in the top chamber were removed with a swab and cells on the lower surface of the membrane were fixed with 4% paraformaldehyde and visualized by staining the nuclei with 4′,6-diamidino-2-phenylindole and a fluorescence microscope. Cell number was counted per multiple fields (n = 4), normalized with respect to the number counted in the presence of vehicle only, and expressed as mean ± standard deviation. For **13**, these data could be fitted to a 3-parameter sigmoidal curve using GraphPad Prism (maximum fixed at 100, EC_{50} = 3.9 ± 0.05 μM, Hill slope = 1.16 ± 0.13, minimum = 16.9 ± 3.6), providing the line shown in Figure 9.

Synthesis. Commercially available reagents and solvents were used without further purification. ^{1}H- and ^{13}C-NMR spectra were recorded on a Bruker 300-, 400- or 500-MHz instrument and chemical shifts were reported in ppm referenced to the deuterated solvent peak. High-resolution mass spectra were obtained with a quadrupole time-of-flight (QTOF) analyzer and electrospray ionization (ESI). Inhibitors were prepared by methods analogous to those previously reported[43] and final compounds used for *in vitro* analysis were of ≥ 95 % purity as judged by the HPLC chromatogram obtained using a Phenomenex C18 reversed-phase column, 4.6 × 150 mm; solvent: acetonitrile/water. An isocratic elution of 40:60 acetonitrile/water or a gradient elution of 75:25 to 30:70 acetonitrile/water over 20 minutes or 80:20 to 30:70 acetonitrile/water with 0.1 % TFA over 15 minutes was used depending on compound. All compounds were eluted with a flow rate of 1.0 mL/min and monitored at UV detector: 260 nm.

General procedure for the synthesis of Cbz-Lys(Acr)-OH compounds ***1, 14-16***.[46] The commercially available Cbz-protected amino acid (1 equiv) was dissolved in THF:1M NaOH (1:1 v/v) and cooled to 0 °C. Sodium hydroxide (1 equiv) and acryloyl chloride (1.2 equiv) were slowly added concurrently. The solution was stirred for 10 min and quenched by the addition of saturated NaCl solution. The mixture was acidified to pH 1 with 1 M HCl and extracted three times with ethyl acetate or dichloromethane. The organic extracts were combined and washed with brine, dried with $MgSO_4$, filtered and concentrated to afford clear, colorless oils.

General procedure for the synthesis of mono-dansylated amine intermediates ***6-9***. The commercially available diamine (6.0 equiv) was dissolved in cooled DCM followed by addition of dansyl chloride (1.0 equiv). The solution was allowed to warm to room temperature and left stirring for 30 min. The solution was washed three times with saturated $NaHCO_3$ solution and the organic phase was washed with brine, dried with $MgSO_4$, filtered and evaporated under reduced

pressure to provide a green/yellow oil. The crude product was purified by flash chromatography over silica gel (elution with gradient of 1-4 % MeOH in CH_2Cl_2) to afford the desired products as yellow/green oils. See supporting information for characterization data.

General procedure for the synthesis of intermediates ***21-29.***[43] Commercially available piperazine (10 equiv) was dissolved in DCM and cooled to 0 ˚C. The sulfonyl chloride (1 equiv) was dissolved in dichloromethane and added slowly via dropping funnel, typically resulting in an opaque solution. The mixture was stirred at 0 ˚C for 30 min and then at room temperature for 1 h. Dilution in DCM followed by addition of saturated $NaHCO_3$ solution gave a clear, colorless solution. The DCM was separated, washed with brine, dried with $MgSO_4$, filtered and concentrated under reduced pressure to afford typically white or yellow solids. See supporting information for characterization data.

General procedure for the synthesis of intermediates ***42, 44*** *starting from acid chlorides.* Boc-piperazine (**39**)[72] (1 equiv) was dissolved in ACN. Triethylamine (2.5 equiv) and the acid chloride (3 equiv) were added dropwise resulting in an opaque solution. The solution was stirred at room temperature for either 1 h or overnight. The solution was concentrated under reduced pressure and the residue was dissolved in DCM. The solution was washed with water, saturated $NaHCO_3$ solution and brine, dried with $MgSO_4$, filtered and concentrated under reduced pressure to afford typically a white or yellow solid. The desired products were used without further purification. See supporting information for characterization data.

General procedure for the synthesis of intermediates ***40, 41, 43-47*** *starting from carboxylic acids.* The carboxylic acid (1 equiv) was dissolved in ACN. EDC•HCl (1 equiv) and NHS (1 equiv) were added and the solution was stirred for 16 h to form the activated ester. N,N-diisopropylethylamine (1 equiv), and Boc-piperazine (**37**)[72] (1 equiv) were added and the

solution was stirred at room temperature for 4 h. The ACN was evaporated under reduced pressure and the residue was dissolved in DCM. The DCM solution was washed with water, saturated $NaHCO_3$ solution and brine and subsequently dried with anhydrous $MgSO_4$. The suspension was filtered and the filtrate was concentrated under reduced pressure to afford typically a white or yellow solid. The desired products were used without further purification. See supporting information for characterization data.

*General Procedure A. Coupling using EDC/NHS to afford irreversible inhibitors **4, 5, 51-56**.* Compound **1** (1 equiv) was dissolved in ACN and EDC•HCl (1 equiv) and NHS (1 equiv) were added. The solution was stirred at room temperature for 16 h. The solution was diluted with ethyl acetate and washed with water, saturated $NaHCO_3$ solution and brine. The ethyl acetate solution was dried with $MgSO_4$, filtered and concentrated to afford the crude NHS ester typically as a white solid. The NHS ester was carried forward without further purification. Crude NHS ester (1.05 equiv) was dissolved in 10 mL ACN. Triethylamine (1 equiv) and the desired amine intermediate (1 equiv) were added and the reaction was left to stir at room temperature for 3 h or kept overnight. The solution was diluted with ethyl acetate, washed with saturated $NaHCO_3$ solution and brine, dried with $MgSO_4$, filtered and concentrated to afford typically white sticky foams.

*General Procedure B. Coupling using EDC/HOBt to afford irreversible inhibitors **10-12, 13, 17-19, 30-38.*** Compound **1** (1 equiv) was added to a solution of EDC•HCl (1.2 equiv), HOBt (1.2 equiv) and N,N-diisopropylethylamine (1.2 equiv) in ACN and stirred at room temperature for 30 min. The amine intermediate (1.2 equiv) was added and the solution was left stirring at room temperature for 20 h. The ACN was evaporated under reduced pressure and the residue was dissolved in $CHCl_3$. The $CHCl_3$ was washed with water, saturated $NaHCO_3$ solution, 1M

HCl and brine. The organic phase was dried with $MgSO_4$, filtered and concentrated under reduced pressure to afford the crude product, typically as an oil. The crude products were purified by flash chromatography over silica gel (elution with a gradient of 0-3 % MeOH in CH_2Cl_2) to afford the desired products mostly as sticky foams.

*General procedure for Boc-deprotection of intermediates **40-48***. Boc-piperizine intermediate (1 equiv) was dissolved in $CHCl_3$ with 10 % v/v trifluoroacetic acid. The solution was stirred at room temperature and monitored via TLC (5 % CH_3OH:DCM with 0.5 % triethylamine). Starting material was no longer detected after approximately 2 h and the $CHCl_3$ was concentrated under reduced pressure. The residue was triturated with diethyl ether and the TFA salt was dissolved in 5 mL of ACN containing one equivalent of trimethylamine and carried forward without further purification.

(S)-6-acrylamido-2-(((benzyloxy)carbonyl)amino)hexanoic acid (**1**). Yield: 900 mg (75 %) of clear, colorless oil. Spectral data matched those from previously reported synthesis.[46] ^{1}H NMR (400 MHz, $CDCl_3$) δ 7.40 – 7.27 (m, 5H), 6.27 (dd, J = 17.0, J = 1.5 Hz, 1H), 6.07 (dd, J = 17.0, 10.3 Hz, 1H), 5.92 (s, 1H), 5.65 – 5.54 (m, 1H), 5.10 (d, J = 2.4 Hz, 2H), 4.36 (t, J = 7.0 Hz, 1H), 3.42 – 3.17 (m, 2H), 1.95 – 1.68 (m, 2H), 1.56 (q, J = 7.5 Hz, 2H), 1.48 – 1.33 (m, 2H).

(S)-2-(6-acrylamido-2-(((benzyloxy)carbonyl)amino)hexanamido)acetic acid (**2**). Compound **5** (100 mg, 0.247 mmol) was dissolved in 10 mL THF and 1 mL of 1 M LiOH was added. The solution was stirred at room temperature and the reaction was monitored via TLC (DCM:MeOH (2%)). After 2 h the solution was concentrated under reduced pressure and 5 mL of water was added. The solution was acidified with 1 M HCl (pH 2) and extracted with ethyl acetate. The ethyl acetate was washed with brine, dried with $MgSO_4$, filtered and concentrated to afford 62 mg (65 %) as a white sticky foam. ^{1}H NMR (400 MHz, CD_3OD) δ 7.50 – 7.05 (m, 5H), 6.21 (d,

J = 5.8 Hz, 1H), 6.20 (d, *J* = 1.3 Hz, 1H), 5.63 (d, *J* = 3.7 Hz, 1H), 5.22 – 5.03 (m, 2H), 4.19 – 4.09 (m, 1H), 4.02 – 3.75 (m, 2H), 3.24 (t, *J* = 6.8 Hz, 2H), 1.86 – 1.82 (m, 1H), 1.70 – 1.65 (m, 1H), 1.62 – 1.49 (m, 1H), 1.47 – 1.38 (m, 2H), ^{13}C NMR (100 MHz, CD_3OD) δ 175.3, 172.7, 168.1, 158.5, 138.1, 132.1, 129.5 128.9, 128.9, 126.5, 67.7, 56.3, 41.7, 40.1, 32.9, 29.9, 24.1; HRMS (ESI-QTOF) m/z $[M + Na]^+$ calcd for $C_{19}H_{25}N_3O_6Na$ 414.1641; found 414.1661.

(S)-benzyl-(1-((5-(dimethylamino)naphthalene)-1-sulfonamido)-10,17-dioxo-3,6-dioxa-9,16-diazanonadec-18-en-11-yl)carbamate (**3**). Compound **3** was prepared according to our previously published synthesis.[51] HRMS (ESI-QTOF) m/z $[M + Na]^+$ calcd for $C_{35}H_{47}N_5O_8SNa$ 720.3043; found 720.3019.

(S)-benzyl-(6-acrylamido-1-amino-1-oxohexan-2-yl)carbamate (**4**). Compound **4** was prepared from ammonium chloride and compound **1** using General Procedure A. In this case, 2 equiv of DABCO was used in place of trimethylamine. The desired compound, 187 mg (54 %) was isolated as a white fluffy powder. mp 156-158 ˚C; ^{1}H NMR (400 MHz, CD_3OD) δ 7.35-7.28 (m, 5H), 6.21-6.19 (m, 2H), 5.63-5.60 (m, 1H), 5.12-5.04 (m, 2H), 4.09-4.06 (m, 1H), 3.23 (t, *J* = 6.9 Hz, 1H), 1.83-1.78 (m, 1H), 1.69-1.61 (m, 1H), 1.56-1.53 (m, 2H), 1.42-1.40 (m, 2H), ^{13}C NMR (100 MHz, CD_3OD) δ 177.7, 168.1, 158.5, 138.1, 132.0, 129.5, 129.0, 128.9, 126.5, 67.7, 56.1, 40.1, 32.9, 29.9, 24.2; HRMS (ESI-QTOF) m/z $[M + Na]^+$ calcd for $C_{17}H_{23}N_3O_4Na$ 356.1586; found 356.1554.

(S)-methyl 2-(6-acrylamido-2-(((benzyloxy)carbonyl)amino)hexanamido)acetate (**5**). Compound **5** was prepared from glycine methyl ester and compound **1** using general coupling procedure A to collect 151 mg (62 %) of the desired product as a white powder. mp 127-129 ˚C; ^{1}H NMR (400 MHz, $CDCl_3$) δ 7.41 – 7.29 (m, 5H), 6.80 (br s, 1H), 6.26 (d, *J* = 16.6 Hz, 1H), 6.08 (dd, *J* = 17.0, 10.2 Hz, 1H), 5.94 (br s, 1H), 5.64 (d, *J* = 7.8 Hz, 1H), 5.58 (br d, *J* = 10.2

Hz, 1H), 5.10 (d, *J* = 1.7 Hz, 2H), 4.26-4.18 (m, 1H), 4.11-3.93 (m, 2H), 3.74 (s, 3H), 3.44 – 3.32 (m, 1H), 2.00 – 1.84 (m, 1H), 1.80 – 1.66 (m, 2H), 1.61 – 1.52 (m, 2H), 1.48 – 1.34 (m, 2H), ^{13}C NMR (100 MHz, $CDCl_3$) δ 172.2, 170.3, 166.0, 156.5, 136.3, 130.9, 128.7, 128.4, 128.2, 126.6, 77.37, 67.3, 52.5, 41.3, 38.7, 31.8, 28.9, 22.2; HRMS (ESI-QTOF) m/z $[M + Na]^+$ calcd for $C_{20}H_{27}N_3O_6Na$ 428.1798; found 428.1799.

(S)-benzyl (6-acrylamido-1-((4-(5-(dimethylamino)naphthalene-1-sulfonamido)butyl)amino)-1-oxohexan-2-yl)carbamate (**10**). Compound **10** was prepared from N-(4-aminobutyl)-5-(dimethylamino)naphthalene-1-sulfonamide (**6**) and compound **1** using General Procedure B to collect 101 mg (26 %) of product as light green crystals. mp 54-56 ˚C; ^{1}H NMR (400 MHz, $CDCl_3$) δ 8.51 (d, *J* = 8.4 Hz, 1H), 8.31 (d, *J* = 8.6 Hz, 1H), 8.18 (d, *J* = 7.3 Hz, 1H), 7.49-7.45 (m, 2H), 7.27 (m, 5H), 7.14 (d, *J* = 7.5 Hz, 1H), 6.68 (brs, 1H), 6.28 (brs, 1H), 6.23 (d, *J* = 16.8 Hz, 1H), 6.07 (m, 1H), 5.98 (brs, 1H), 5.88 (brs, 1H), 5.52 (d, *J* = 10.3 Hz, 1H), 5.03 (s, 2H), 4.10 (m, 1H), 3.25 (m, 2H), 3.10 (m, 2H), 2.85 (s, 6H), 2.81 (m, 2H), 1.78 (m, 1H), 1.64 (m, 1H), 1.50 (m, 2H), 1.40 (m, 6H), 1.23 (m, 1H), ^{13}C NMR (100 MHz, $CDCl_3$) δ 172.3, 166.3, 156.6, 152.0, 136.4, 135.1, 131.0, 130.5, 130.0, 129.8, 129.6, 128.5, 126.7, 123.4, 119.2, 115.4, 67.2, 55.1, 45.6, 43.0, 39.0, 32.2, 29.0, 26.9, 26.6, 22.6; HRMS (ESI-QTOF) m/z $[M + Na]^+$ calcd for $C_{33}H_{43}N_5O_6SNa$ 660.2833; found 660.2842.

(S)-benzyl (6-acrylamido-1-((3-(5-(dimethylamino)naphthalene-1-sulfonamido)propyl)amino)-1-oxohexan-2-yl)carbamate (**11**). Compound **11** was prepared from N-(3-aminopropyl)-5-(dimethylamino)naphthalene-1-sulfonamide (**7**) and compound **1** using General Procedure B to afford 158 mg (36 %) of the product as light green crystals. mp 65-67 ˚C; ^{1}H NMR (400 MHz, $CDCl_3$) δ 8.46-8.43 (d *J* = 8.5 Hz, 1H), 8.26-8.24 (d, *J* = 8.6 Hz, 1H), 8.14-8.12 (dd, *J* = 7.3 Hz, *J* = 1.2 Hz, 1H), 7.49-7.41 (m, 2H), 7.27-7.21 (m, 5H), 7.10-7.08 (d, *J* = 7.5 Hz, 1H), 6.61-6.59

(m, 1H), 6.18-6.13 (d, *J* = 16.9 Hz, 1H), 6.02-5.95 (dd, *J* = 16.9 Hz, 10.z Hz, 1H), 5.94-5.89 (m, 1H), 5.58-5.56 (d, *J* = 7.5 Hz, 1H), 5.49-5.46 (d, *J* = 10.2 Hz, 1H), 5.04-4.95 (m, 2H), 4.03-3.98 (m, 1H), 3.29-3.13 (m, 4H), 2.86-2.77 (m, 8H), 1.75-1.65 (m, 1H), 1.57-1.39 (m, 5H), 1.32-1.21 (m, 2H), ^{13}C NMR (100 MHz, $CDCl_3$) δ 172.5, 166.0, 151.9, 136.2, 135.2, 130.7, 130.3, 129.9, 129.6, 129.2, 128.5, 128.3, 128.2, 128.1, 128.0, 126.6, 123.2, 119.0, 115.2, 67.0, 54.9, 45.4, 40.3, 38.6, 36.3, 31.7, 29.6, 28.9, 22.3; HRMS (ESI-QTOF) m/z $[M + Na]^+$ calcd for $C_{32}H_{41}N_5O_6SNa$ 646.2675; found 646.2657.

(S)-benzyl (6-acrylamido-1-((2-(5-(dimethylamino)naphthalene-1-sulfonamido)ethyl)amino)-1-oxohexan-2-yl)carbamate (**12**). Compound **12** was prepared from N-(2-aminoethyl)-5-(dimethylamino)naphthalene-1-sulfonamide (**8**) and compound **1** using General Procedure B to collect 89 mg (21 %) of the product as a yellow/green sticky foam. ^{1}H NMR (400 MHz, $CDCl_3$) δ 8.50 (d, *J* = 8.5 Hz, 1H), 8.27 (d, *J* = 8.6 Hz, 1H), 8.15 (d, *J* = 7.1 Hz, 1H), 7.46 (m, 2H), 7.26 (m, 5H), 7.11 (d, *J* = 7.4 Hz, 1H), 6.55 (m, 1H), 6.50 (m, 1H), 6.21-6.16 (dd, *J* = 16.9 Hz, 1.5 Hz, 1H), 6.10-6.03 (dd, *J* = 10.0 Hz, 16.9 Hz, 1H), 5.95 (d, *J* = 7.4 Hz, 1H), 5.49-5.46 (dd, *J* = 10.0 Hz, 1.5 Hz, 1H), 5.04-5.01 (m, 2H), 4.09 (m, 1H), 3.25 (m, 4H), 2.96 (m, 2H), 2.83 (s, 6H), 1.75 (m, 1H), 1.64 (m, 1H), 1.47 (m, 2H), 1.34 (m, 2H), ^{13}C NMR (100 MHz, $CDCl_3$) δ 172.9, 166.3, 156.6, 136.3, 135.0, 130.9, 130.6, 129.7, 129.5, 128.7, 128.5, 128.4, 128.3, 126.7, 123.5, 119.2, 115.6, 67.3, 55.1, 45.6, 42.9, 39.5, 38.9, 32.0, 29.0, 22.6; HRMS (ESI-QTOF) m/z $[M + Na]^+$ calcd for $C_{31}H_{39}N_5O_6SNa$ 632.2519; found 632.2526.

(S)-benzyl-(6-acrylamido-1-(4-((5-(dimethylamino)naphthalen-1-yl)sulfonyl)piperazin-1-yl)-1-oxohexan-2-yl)carbamate (**13**). Compound **13** was prepared according to our recently published synthesis.[60] HRMS (ESI-QTOF) m/z $[M + Na]^+$ calcd for $C_{33}H_{41}N_5O_6SNa$ 658.2675; found 658.2657.

(S)-3-acrylamido-2-(((benzyloxy)carbonyl)amino)propanoic acid (**14**). Collected 240 mg (72 %) as a clear, colorless oil. ^{1}H NMR (400 MHz, CD_3OD) δ 7.37-7.27 (m, 5H), 6.22-6.20 (m, 2H), 5.67-5.64 (m, 1H), 5.09-5.08 (m, 2H), 4.38-4.35 (m, 1H), 3.77-3.73 (m, 1H), 3.59-3.54 (m, 1H), ^{13}C NMR (100 MHz, CD_3OD) δ 173.4, 168.8, 158.5, 138.1, 131.7, 129.4, 129.0, 128.8, 127.1, 67.7, 55.5, 41.7; HRMS (ESI-TOF) m/z $[M + Na]^+$ calcd for $C_{14}H_{16}N_2O_5Na$ 315.0957; found 315.0945.

(S)-4-acrylamido-2-(((benzyloxy)carbonyl)amino)butanoic acid (**15**). Collected 165 mg (64 %) as a clear, colorless oil. ^{1}H NMR (400 MHz, $CDCl_3$) δ 9.44 (br s, 1H), 7.26-7.19 (m, 5H), 7.08-7.03 (m, 1H), 6.18-6.13 (d, *J* = 16.9 Hz, 1H), 6.06-6.00 (dd, *J* = 16.9 Hz, *J* = 10.4 Hz, 1H), 5.98-5.95 (m, 1H), 5.54-5.52 (d, *J* = 10.4 Hz, 1H), 4.99 (s, 2H), 4.28-4.24 (m, 1H), 3.57-3.51 (m, 1H), 3.07-3.02 (m, 1H), 2.05-1.97 (m, 1H), 1.80-1.71 (m, 1H), ^{13}C NMR (100 MHz, $CDCl_3$) δ 174.2, 167.2, 156.8, 136.1, 130.4, 128.7, 128.3, 128.1, 127.5, 67.3, 51.7, 36.2, 32.7, 29.3; HRMS (ESI-TOF) m/z $[M + Na]^+$ calcd for $C_{15}H_{18}N_2O_5Na$ 329.1113; found 329.1103.

(S)-5-acrylamido-2-(((benzyloxy)carbonyl)amino)pentanoic acid (**16**). Collected 254 mg (67 %) as a clear colorless oil. ^{1}H NMR (400 MHz, CD_3OD) δ 7.34-7.27 (m, 5H), 6.22-6.19 (m, 2H), 5.64-5.61 (m, 1H), 2.08 (s, 2H), 4.19-4.15 (m, 1H), 3.28-3.24 (t, *J* = 6.8 Hz, 2H), 1.93-1.83 (m, 1H), 1.74-1.57 (m, 3H), ^{13}C NMR (100 MHz, CD_3OD) δ 175.6, 168.1, 158.6, 138.1, 131.9, 129.4, 128.9, 128.7, 126.6, 67.6, 55.1, 39.9, 30.1, 26.8; HRMS (ESI-TOF) m/z $[M + Na]^+$ calcd for $C_{16}H_{20}N_2O_5Na$ 343.1270; found 343.1272.

(S)-benzyl (3-acrylamido-1-(4-((5-(dimethylamino)naphthalen-1-yl)sulfonyl)piperazin-1-yl)-1-oxopropan-2-yl)carbamate (**17**). Compound **17** was prepared from N,N-dimethyl-5-(piperazin-1-ylsulfonyl)naphthalen-1-amine (**9**) and acrylamide **14** using General Procedure B to afford 58 mg (32 %) of the final compound as a yellow/green sticky foam. ^{1}H NMR (400 MHz, $CDCl_3$) δ

8.83-8.71 (m, 1H), 8.49-8.41 (m, 1H), 8.24-8.23 (d, *J* = 7.2 Hz, 1H), 7.66-7.54 (m, 2H), 7.36-7.26 (m, 6H), 6.27-6.15 (m, 2H), 6.04-5.95 (m, 1H), 5.88-5.84 (m, 1H), 5.61-5.59 (d, *J* = 10.2 Hz, 1H), 5.04 (s, 2H) , 4.76-4.70 (m, 1H), 3.73-3.56 (m, 5H), 3.38-3.15 (m, 5H), 2.99 (s, 6H), ^{13}C NMR (100 MHz, $CDCl_3$) δ 168.3, 166.30, 156.3, 152.0, 136.1, 132.4, 131.2, 130.9, 130.3, 130.2, 128.6, 128.5, 128.4, 128.2, 127.2, 123.3, 119.4, 115.5, 67.3, 50.8, 45.6, 45.5, 45.3, 45.1, 42.6, 41.9 ; HRMS (ESI-QTOF) m/z $[M + Na]^+$ calcd for $C_{30}H_{35}N_5O_6SNa$ 616.2206; found 616.2194.

(S)-benzyl (4-acrylamido-1-(4-((5-(dimethylamino)naphthalen-1-yl)sulfonyl)piperazin-1-yl)-1-oxobutan-2-yl)carbamate (**18**). Compound **18** was prepared from N,N-dimethyl-5-(piperazin-1-ylsulfonyl)naphthalen-1-amine (**9**) and acrylamide **15** using General Procedure B to afford 117 mg (26 %) of the final compound as a yellow/green sticky foam. ^{1}H NMR (400 MHz, $CDCl_3$) δ 8.59-8.57 (d, *J* = 8.5 Hz, 1H), 8.32-8.29 (d, *J* = 8.7 Hz, 1H), 8.20-8.18 (d, *J* = 7.2 Hz, 1H), 7.56-7.52 (m, 2H), 7.19-7.18 (d, *J* = 7.5 Hz, 1H), 6.62-6.57 (m, 1H), 6.25-6.21 (d, *J* = 16.5 Hz, 1H), 6.11-6.05 (dd, *J* = 16.5 Hz, 10.2 Hz, 1 H), 5.90-5.88 (d, *J* = 7.8 Hz, 1H), 5.63-5.61 (d, *J* = 10.2 Hz, 1H), 5.06 (s, 2H), 4.59-4.49 (m, 1H), 3.75-3.67 (m, 2H), 3.58-3.50 (m, 1H), 3.41-3.33 (m, 2H), 3.28-3.10 (m, 4H), 3.01-2.92 (m, 1H), 2.88 (s, 6H), 1.97-1.87 (m, 1H), 1.56-1.45 (m, 1H), ^{13}C NMR (100 MHz, $CDCl_3$) δ 170.0, 165.8, 156.9, 152.0, 136.1, 132.3, 131.3, 130.9, 130.3, 130.2, 128.7, 128.5, 128.4, 128.1, 126.7, 123.3, 119.3, 115.6, 67.3, 48.5, 45.6, 45.5, 45.2, 45.1, 41.8, 35.6, 33.2; HRMS (ESI-QTOF) m/z $[M + H]^+$ calcd for $C_{31}H_{38}N_5O_6S$ 608.2543; found 608.2549.

(S)-benzyl (5-acrylamido-1-(4-((5-(dimethylamino)naphthalen-1-yl)sulfonyl)piperazin-1-yl)-1-oxopentan-2-yl)carbamate (**19**) Compound **19** was prepared from N,N-dimethyl-5-(piperazin-1-ylsulfonyl)naphthalen-1-amine (**9**) and acrylamide **16** using General Procedure B to afford 39 mg

(23 %) of the final compound as a yellow/green solid. mp 69-70 ˚C; ^{1}H NMR (400 MHz, CDCl3) δ 8.53-8.51 (d, *J* = 8.5 Hz, 1H), 8.27-8.24 (d, *J* = 8.5 Hz, 1H), 8.14-8.12 (dd, *J* = 7.3, 1.0 Hz, 1H), 7.49-7.45 (m, 2H), 7.28-7.21 (m, 5H), 7.13-7.11 (d, *J* = 7.2 Hz, 1H), 6.19-6.15 (dd, *J* = 17.0, 1.3 Hz, 1H), 6.01-5.94 (dd, *J* = 17.0, 10.2 Hz, 1H), 5.89-5.84 (m, 1H), 5.60-5.57 (d, *J* = 8.4 Hz, 1H). 5.55-5.52 (dd, *J* = 10.2, 1.3 Hz, 1H), 4.97 (s, 2H), 4.55-4.50 (m, 1H), 3.51-3.37 (m, 3H), 3.32-3.18 (m, 4H), 3.11-2.98 (m, 3H), 2.82 (s, 6H), 1.58-1.42 (m, 4H), ^{13}C NMR (100 MHz, $CDCl_3$) δ 170.3, 165.7, 156.3, 152.0, 136.2, 132.4, 131.3, 131.0, 130.9, 130.4, 130.2, 128.7, 128.5, 128.3, 128.2, 126.7, 123.3, 119.4, 115.5, 67.2, 50.2, 45.7, 45.5, 45.3, 41.9, 39.0, 31.2, 24.9; HRMS (ESI-QTOF) m/z [M + Na]+ calcd for $C_{32}H_{41}N_5O_6SNa$ 646.2675; found 646.2657.

(S)-benzyl 6-acrylamido-1-(4-(naphthalen-1-ylsulfonyl)piperazin-1-yl)-1-oxohexan-2-yl-carbamate (**30**).

Compound **30** was prepared from 1-(naphthalen-1-ylsulfonyl)piperazine (**21**) and compound **1** using General Procedure B to afford 100 mg (23 %) of the desired product as a white foam. mp 59-61 ˚C; ^{1}H NMR (400 MHz, $CDCl_3$) δ 8.70 (d, *J* = 8.7 Hz, 1H), 8.22 (dd, *J* = 7.4, *J* = 1.2 Hz, 1H), 8.10 (d, *J* = 8.2 Hz, 1H), 7.97 – 7.91 (m, 1H), 7.71 – 7.53 (m, 3H), 7.39 – 7.27 (m, 5H), 6.24 (dd, *J* = 17.0, 1.5 Hz, 1H), 6.04 (dd, *J* = 17.0, 10.2 Hz, 1H), 5.74 (br s, 1H), 5.67 – 5.56 (m, 2H), 5.03 (s, 2H), 4.51 (td, *J* = 8.4, 4.3 Hz, 1H), 3.87 – 3.79 (m, 1H), 3.58 (d, *J* = 5.1 Hz, 1H), 3.47 (dt, *J* = 12.9, 9.3 Hz, 2H), 3.39 – 3.19 (m, 4H), 3.13 – 3.00 (m, 2H), 1.65 – 1.46 (m, 4H), 1.38 – 1.23 (m, 2H), ^{13}C NMR (100 MHz, $CDCl_3$) δ 170.4, 165.7, 156.2, 136.3, 135.1, 134.6, 132.2, 131.0, 130.9, 129.2, 128.9, 128.7, 128.5, 128.4, 128.1, 127.2, 126.5, 124.9, 124.3, 67.1, 50.3, 45.8, 45.4, 45.3, 41.8, 39.1, 32.9, 28.9, 22.3; HRMS (ESI-QTOF) m/z $[M + Na]^+$ calcd for $C_{31}H_{36}N_4O_6SNa$ 615.2253; found 615.2232.

(S)-benzyl (6-acrylamido-1-(4-(naphthalen-2-ylsulfonyl)piperazin-1-yl)-1-oxohexan-2-yl)-carbamate (**31**).

Compound **31** was prepared from 1-(naphthalen-2-ylsulfonyl)piperazine (**22**) and compound **1** using General Procedure B to collect 102 mg (24 %) of the desired product as a white foam. mp 65-66 ˚C; ^{1}H NMR (400 MHz, $CDCl_3$) δ 8.33 (d, *J* = 1.7 Hz, 1H), 7.99 (d, *J* = 8.2 Hz, 2H), 7.92 (d, *J* = 7.6 Hz, 1H), 7.72 (dd, *J* = 8.7, 1.8 Hz, 1H), 7.65 (dd, *J* = 6.9, 1.5 Hz, 2H), 7.35 – 7.27 (m, 5H), 6.24 (dd, *J* = 17.0, 1.5 Hz, 1H), 6.03 (dd, *J* = 17.0, 10.3 Hz, 1H), 5.70 (t, *J* = 5.8 Hz, 1H), 5.59 (dd, *J* = 10.2, 1.5 Hz, 2H), 4.99 (d, *J* = 1.8 Hz, 2H), 4.51 (td, *J* = 8.4, 4.2 Hz, 1H), 3.95-3.85 (m, 1H), 3.68-3.61 (m, 1H), 3.52 (dt, *J* = 13.8, 10.3 Hz, 2H), 3.24 (qd, *J* = 13.5, 6.6 Hz, 4H), 3.05 – 2.81 (m, 2H), 1.63 – 1.42 (m, 4H), 1.43 – 1.15 (m, 2H), ^{13}C NMR (100 MHz, $CDCl_3$) δ 170.4, 165.7, 156.2, 136.3, 135.2, 132.6, 132.3, 130.9, 129.7, 129.4, 129.3, 129.3, 128.7, 128.3, 128.1, 128.1, 127.9, 126.5, 122.8, 67.1, 50.3, 46.3, 45.9, 45.2, 41.7, 39.1, 32.9, 28.9, 22.3; HRMS (ESI-QTOF) m/z $[M + Na]^+$ calcd for $C_{31}H_{36}N_4O_6SNa$ 615.2249; found 615.2253.

(S)-benzyl (6-acrylamido-1-oxo-1-(4-(phenylsulfonyl)piperazin-1-yl)hexan-2-yl)carbamate (**32**).

Compound **32** was prepared from 1-(phenylsulfonyl)piperazine (**23**) and compound **1** using General Procedure B to collect 82 mg (20 %) of the desired product as a sticky, white foam. ^{1}H NMR (400 MHz, $CDCl_3$) δ 7.77 – 7.72 (m, 2H), 7.65 – 7.60 (m, 1H), 7.58 – 7.52 (m, 2H), 7.36 – 7.29 (m, 5H), 6.26 (dd, *J* = 17.0, 1.5 Hz, 1H), 6.05 (dd, *J* = 16.9, 10.3 Hz, 1H), 5.68 (s, 1H), 5.64 – 5.58 (m, 2H), 5.05 (s, 2H), 4.54 (td, *J* = 8.5, 4.2 Hz, 1H), 3.92 (d, *J* = 13.4 Hz, 1H), 3.65 (s, 1H), 3.53 (d, *J* = 18.2 Hz, 2H), 3.28 (qd, *J* = 18.4, 16.0, *J* = 9.3 Hz, 4H), 2.88 (dd, *J* = 21.5, 10.4 Hz, 2H), 1.67 – 1.47 (m, 3H), 1.36 (q, *J* = 7.3 Hz, 2H), ^{13}C NMR (100 MHz, $CDCl_3$) δ 170.4, 165.7, 156.3, 136.3, 135.5, 133.4, 130.9, 129.5, 128.7, 128.4, 128.1, 127.8, 126.5, 67.1, 50.3,

46.2, 45.9, 45.1, 41.6, 39.1, 32.9, 28.9, 22.3; HRMS (ESI-QTOF), m/z [M + Na]$^+$ calcd for $C_{27}H_{34}N_4O_6SNa$ 565.2097; found 565.2094.

(S)-benzyl (6-acrylamido-1-(4-(benzylsulfonyl)piperazin-1-yl)-1-oxohexan-2-yl)carbamate (**33**).

Compound **33** was prepared from 1-(benzylsulfonyl)piperazine (**24**) and compound **1** using General Procedure B to collect 96 mg (23 %) of the desired product as a white foam. mp 50-52 °C; ^{1}H NMR (400 MHz, $CDCl_3$) δ 7.41 – 7.29 (m, 10H), 6.25 (dd, *J* = 17.0, 1.5 Hz, 1H), 6.07 (dd, *J* = 17.0, 10.2 Hz, 1H), 5.86 (t, *J* = 5.9 Hz, 1H), 5.74 (d, *J* = 8.4 Hz, 1H), 5.60 (dd, *J* = 10.3, 1.5 Hz, 1H), 5.08 (d, *J* = 1.3 Hz, 2H), 4.55 (td, *J* = 8.4, 4.4 Hz, 1H), 4.23 (s, 2H), 3.72 – 3.66 (m, 1H), 3.53 – 3.45 (m, 1H), 3.44 – 3.24 (m, 4H), 3.20 – 3.11 (m, 2H), 3.01 (dtt, *J* = 20.5, 8.7, 3.7 Hz, 2H), 1.63 (ddd, *J* = 12.0, 5.7, 2.8 Hz, 1H), 1.57 – 1.50 (m, 3H), 1.37 (q, *J* = 7.5 Hz, 2H), ^{13}C NMR (100 MHz, $CDCl_3$) δ 170.5, 165.7, 156.25, 136.3, 130.9, 130.8, 129.2, 129.0, 128.7, 128.5, 128.4, 128.1, 126.4, 67.1, 57.5, 50.3, 46.1, 45.8, 42.3, 39.0, 32.8, 28.9, 22.3; HRMS (ESI-QTOF) m/z [M + Na]$^+$ calcd for $C_{28}H_{36}N_4O_6SNa$ 579.2253; found 579.2299.

(S)-benzyl (6-acrylamido-1-(4-(cyclohexylsulfonyl)piperazin-1-yl)-1-oxohexan-2-yl)carbamate (**34**). Compound **34** was prepared from 1-(cyclohexylsulfonyl)piperazine (**25**) and compound **1** using General Procedure B to collect 88 mg (21 %) of the desired product as a sticky, white foam. ^{1}H NMR (400 MHz, $CDCl_3$) δ 7.39 – 7.30 (m, 5H), 6.27 (dd, *J* = 17.0, 1.5 Hz, 1H), 6.07 (dd, *J* = 17.0, 10.3 Hz, 1H), 5.75 (br s, 1H), 5.71 (d, *J* = 8.5 Hz, 1H), 5.62 (dd, *J* = 10.3, 1.5 Hz, 1H), 5.09 (s, 2H), 4.62 (td, *J* = 8.4, 4.4 Hz, 1H), 3.81 (br s, 1H), 3.61 (br s, 1H), 3.56 – 3.40 (m, 4H), 3.35 – 3.24 (m, 2H), 2.94 – 2.87 (m, 1H), 2.10 (d, *J* = 13.0 Hz, 2H), 1.89 (d, *J* = 13.3 Hz, 2H), 1.73 – 1.67 (m, 2H), 1.61 – 1.33 (m, 7H), 1.31 – 1.16 (m, 3H), ^{13}C NMR (100 MHz, $CDCl_3$) δ 170.6, 165.7, 156.3, 136.3, 130.9, 128.7, 128.4, 128.2, 126.5, 67.2, 61.9, 50.4, 46.5,

46.3, 46.2, 42.8, 39.1, 33.0, 29.0, 26.7, 25.3, 25.2, 22.3; HRMS (ESI-QTOF) m/z $[M + Na]^+$ calcd for $C_{27}H_{40}N_4O_6SNa$ 571.2566; found 571.2544.

(S)-benzyl(6-acrylamido-1-(4-(isopropylsulfonyl)piperazin-1-yl)-1-oxohexan-2-yl)carbamate (**35**). Compound **35** was prepared from 1-(isopropylsulfonyl)piperazine (**26**) and compound **1** using General Procedure B to collect 115 mg (29 %) of the desired product as white crystals. mp 48-49 ˚C; ^{1}H NMR (400 MHz, $CDCl_3$) δ 7.40 – 7.29 (m, 5H), 6.26 (dd, *J* = 17.0, 1.5 Hz, 1H), 6.07 (dd, *J* = 17.0, 10.2 Hz, 1H), 5.80 (s, 1H), 5.73 (d, *J* = 8.4 Hz, 1H), 5.61 (dd, *J* = 10.3, 1.5 Hz, 1H), 5.09 (s, 2H), 3.87 – 3.78 (m, 1H), 3.61 (s, 1H), 3.57 – 3.22 (m, 8H), 3.18 (p, *J* = 6.8 Hz, 1H), 1.76 (s, 1H), 1.71 – 1.66 (m, 1H), 1.62 – 1.54 (m, 3H), 1.43-1.36 (m, 1H), 1.35 (s, 3H), 1.33 (s, 3H), ^{13}C NMR (100 MHz, $CDCl_3$) δ 170.6, 165.7, 156.3, 136.3, 130.9, 128.7, 128.4, 128.2, 126.5, 67.2, 53.8, 50.4, 46.5, 46.3, 46.2, 42.8, 39.1, 32.9, 29.0, 22.3, 16.9; HRMS (ESI-QTOF) m/z $[M + Na]^+$ calcd for $C_{24}H_{36}N_4O_6SNa$ 561.2253; found 531.2241.

(S)-benzyl (6-acrylamido-1-(4-(ethylsulfonyl)piperazin-1-yl)-1-oxohexan-2-yl)carbamate (**36**) Compound **36** was prepared from 1-(ethylsulfonyl)piperazine (**27**) and compound **1** using General Procedure B to collect 102 mg (22%) of the desired product as a clear, colorless oil. ^{1}H NMR (400 MHz, $CDCl_3$) δ 7.41 – 7.30 (m, 5H), 6.26 (dd, *J* = 17.0, 1.5 Hz, 1H), 6.06 (dd, *J* = 17.0, 10.2 Hz, 1H), 5.74 (br s, 1H), 5.70 (d, *J* = 8.4 Hz, 1H), 5.62 (dd, *J* = 10.2, 1.5 Hz, 1H), 5.09 (d, *J* = 1.8 Hz, 2H), 4.62 (td, *J* = 8.4, 4.5 Hz, 1H), 3.86 (br s, 1H), 3.66 (br s, 1H), 3.60 – 3.54 (m, 2H), 3.44 – 3.17 (m, 6H), 2.96 (q, *J* = 7.4 Hz, 2H), 1.79 – 1.65 (m, 1H), 1.66 – 1.50 (m, 3H), 1.45 – 1.33 (m, 5H); ^{13}C NMR (100 MHz, $CDCl_3$) δ 170.8, 168.4, 165.9, 156.4, 151.7, 149.9, 136.4, 135.0, 131.1, 128.7, 128.2, 126.3, 69.1, 68.0, 67.1, 59.7, 53.2, 50.5, 46.0, 45.8, 45.6, 44.5, 42.3, 39.0, 32.7, 29.1, 23.7, 22.4, 20.4, 7.9; HRMS (ESI-QTOF) m/z [M + Na]+ calcd for $C_{23}H_{34}N_4O_6NaS$ 517.2097; found 517.2140.

(S)-benzyl(6-acrylamido-1-(4-(methylsulfonyl)piperazin-1-yl)-1-oxohexan-2-yl)carbamate (**37**) Compound **37** was prepared from 1-(methylsulfonyl)piperazine (**28**) and compound 1 using General Procedure B to collect 93 mg (26 %). ^{1}H NMR (400 MHz, $CDCl_3$) δ 7.38-7.30 (m, 5H), 6.25 (dd, J = 17.0, 1.5 Hz, 1H), 6.06 (dd, J = 17.0, 10.2 Hz, 1H), 5.78 (bs, 1H), 5.71 (d, J = 8.3 Hz, 1H), 5.62 (dd, J = 10.2, 1.5 Hz, 1H), 5.08 (d, J = 2.3 Hz, 2H), 4.62 (td, J = 8.3, J = 4.6 Hz, 1H), 3.89-3.82 (m, 1H), 3.73-3.66 (m, 1H), 3.63-3.55 (m, 2H), 3.37 – 3.24 (m, 4H), 3.23-3.10 (m, 2H), 2.80 (s, 3H), 1.77 – 1.66 (m, 2H), 1.64 – 1.50 (m, 3H), 1.39 (p, J = 7.5 Hz, 2H); ^{13}C NMR (100 MHz, $CDCl_3$) δ 170.7, 165.8, 156.3, 136.3, 130.0, 128.7, 128.4, 128.2, 126.5, 67.2, 50.4, 45.0, 45.6, 45.4, 41.9, 38.9, 35.1, 32.8, 29.1, 22.3; HRMS (ESI-QTOF) m/z $[M + Na]^+$ calcd for $C_{22}H_{32}N_4NaO_6S$ 503.1940; found 503.1947.

(S)-benzyl(6-acrylamido-1-oxo-1-(4-(thiophen-2-ylsulfonyl)piperazin-1-yl)hexan-2-yl)carbamate (**38**). Compound **38** was prepared from 1-(thiophen-2ylsulfonyl)piperazine (**29**) and compound **1** using General Procedure B to collect 39 mg (8 %) of the desired product as a clear oil; ^{1}H NMR (400 MHz, $CDCl_3$) δ 7.64 – 7.63 (dd, *J* = 5.0, 1.2 Hz, 1H), 7.53 – 7.52 (dd, *J* = 3.7, 1.1 Hz, 1H), 7.36 – 7.28 (m, 5H), 7.16 – 7.13 (dd, *J* = 5.0, 3.8 Hz, 1H), 6.26 – 6.22 (dd, *J* = 17.0, 1.5 Hz, 1H), 6.09 – 6.02 (dd, *J* = 17.0, 10.2 Hz, 1H), 5.96 (s, 1H), 5.76 – 5.74 (d, *J* = 8.4 Hz, 1H), 5.60 – 5.58 (dd, *J* = 10.2, 1.4 Hz, 1H) 5.04 (s, 2H), 4.57 – 4.52 (m, 1H), 3.93 – 3.89 (m, 1H), 3.70 – 3.67 (m, 1H), 3.57 – 3.46 (m, 2H), 3.33 – 3.17 (m, 4H), 2.96 – 2.85 (m, 2H), 1.96 (s, 1H), 1.67 – 1.58 (m, 1H), 1.54 – 1.44 (m, 3H), 1.37 – 1.30 (m, 2H); ^{13}C NMR (100 MHz, $CDCl_3$) δ 170.5, 165.8, 156.3, 136.2, 135. 5, 133.0, 132.9, 130.9, 128.6, 128.3, 128.1, 128.0, 126.4, 67.1, 50.3, 46.2, 45.8, 44.9, 41.4, 39.0, 32.8, 29.7, 28.9, 22.3; HRMS (ESI-QTOF) m/z $[M + Na]^+$ calcd for $C_{25}H_{32}N_4O_6NaS_2$ 571.1661; found 571.1626.

(S)-benzyl (1-(4-(1-naphthoyl)piperazin-1-yl)-6-acrylamido-1-oxohexan-2-yl)carbamate (**AA9**/**49**). Compound **49** was prepared from Boc-deprotected **40** and compound **1** using General Procedure B to collect 254 mg (41 %) of the desired product as a white sticky foam. ^{1}H NMR (500 MHz, $(CD_3)_2SO$) at 120 ºC) δ 7.99-7.96 (m, 2H), 7.84-7.81 (m, 2H), 7.59-7.54 (m, 3H), 7.46-7.44 (m, 2H), 7.35-7.26 (m, 4H), 6.74-6.72 (d, *J* = 7.5 Hz, 1H), 6.21-6.16 (dd, *J* = 17.1, 10.3 Hz, 1H), 6.05-6.01 (dd, *J* = 17.1, 2.1 Hz, 1H), 5.51-5.48 (dd, *J* = 10.3, 2.1 Hz, 1H), 5.04 (s, 1H), 4.46-4.41 (m, 1H), 3.63-3.38 (m, 8H), 3.16-3.12 (q, *J* = 6.85 Hz, 2 Hz), 1.71-1.56 (m, 2H), 1.51-1.44 (m, 2H), 1.39-1.29 (m, 2H), ^{13}C NMR (100 MHz, $(CD_3)_2SO$) δ169.9, 167.8, 164.1, 155.0, 136.5, 133.5, 132.6, 131.7, 128.7, 128.2, 127.6, 127.5, 126.9, 126.8, 126.2, 125.6, 124.5, 123.9, 123.2, 123.1, 65.0, 50.3, 42.7, 37.8, 30.8, 28.2, 21.9; HRMS (ESI-QTOF) m/z $[M + Na]^+$ calcd for $C_{32}H_{36}N_4O_5Na$ 579.2584; found 579.2574.

(S)-benzyl(1-(4-(2-naphthoyl)piperazin-1-yl)-6-acrylamido-1-oxohexan-2-yl)carbamate (**AA10/50**). Compound **50** was prepared from Boc-deprotected **41** and compound **1** using General Procedure B to collect 195 mg (36 %) of the desired product as a white sticky foam. ^{1}H NMR (300 MHz, $(CD_3)_2SO$ at 120 ˚C) δ 7.99-7.92 (m, 4H), 7.74 (br s, 1H), 7.60-7.48 (m, 3H), 7.33-7.23 (m, 5H), 7.06 (br s, 1H), 6.22-6.13 (dd, *J* = 17.2, 10.1 Hz, 1H), 6.06-5.99 (dd, *J* = 17.2, 2.4 Hz, 1H), 5.67 (s, 1H), 5.52-5.47 (dd, *J* = 10.1, 2.4 Hz, 1H), 5.02 (s, 2H), 4.46-4.38 (m, 1H), 3.63-3.46 (m, 8H), 3.14-3.07 (m, 2H), 1.65-1.53 (m, 2H), 1.49-1.39 (m, 2H), 1.36-1.25 (m, 2H), δ ^{13}C NMR (75 MHz, $(CD_3)_2SO$) 170.9, 169.8, 165.1, 137.6, 133.7, 133.6, 132.8, 132.6, 128.7, 128.6, 128.5, 128.1, 128.0, 127.5, 127.1, 126.9, 124.8, 124.6, 66.0, 55.1, 51.2, 38.8, 31.7, 29.3, 23.1; HRMS (ESI-QTOF) m/z $[M + Na]^+$ calcd for $C_{32}H_{36}N_4O_5Na$ 579.2584; found 579.2557.

(S)-benzyl (5-acrylamido-1-(4-benzoylpiperazin-1-yl)-1-oxopentan-2-yl)carbamate (**51**). Compound **51** was prepared from Boc-deprotected **40** and compound **1** using General Procedure

A to collect 151 mg (31 %) of the desired product as a white, sticky foam. ^{1}H NMR (300 MHz, $(CD_3)_2SO$ at 80 ˚C) δ 7.73-7.65 (br s, 1H), 7.44-7.22 (m, 10 H), 7.05-6.98 (br s, 1H), 6.17-6.09 (dd, *J* = 17.1, 10.0 Hz, 1H), 6.01-5.95 (dd, *J* = 17.1, 2.3 Hz, 1H), 5.47-5.44 (dd, *J* = 10.0, 2.3 Hz, 1H), 4.97 (s, 2H), 4.41-4.36 (m, 1H), 3.55-3.36 (m, 8H), 3.09-3.02 (m, 2H), 1.61-1.49 (m, 2H), 1.44-1.33 (m, 2H), 1.32-1.20 (m, 2H), ^{13}C NMR (75 MHz, $(CD_3)_2SO$ at 80 ˚C) δ 170.1, 168.9, 164.2, 136.7, 135.4, 131.7, 129.1, 127.9, 127.8, 127.2, 127.1, 126.4, 123.7, 65.1, 50.3, 37.9, 30.8, 28.3, 22.2; HRMS (ESI-QTOF) m/z $[M + Na]^+$ calcd for $C_{28}H_{34}N_4O_5Na$ 529.2427; found 529.2433.

(S)-benzyl (6-acrylamido-1-oxo-1-(4-(2-phenylacetyl)piperazin-1-yl)hexan-2-yl)carbamate(**52**).

Compound **52** was prepared from Boc-deprotected **43** and compound **1** using General Procedure A to collect 36 mg (21 %) of the desired product as a whit solid. mp 48-49 °C; ^{1}H NMR (400 MHz, $CDCl_3$) δ 7.41 – 7.29 (m, 7H), 7.24 (d, J = 7.1 Hz, 3H), 6.25 (dd, J = 17.0, 1.5 Hz, 1H), 6.06 (dd, J = 17.0, 10.2 Hz, 1H), 5.78 (br s, 1H), 5.70 (d, J = 8.4 Hz, 1H), 5.60 (dd, J = 10.5, 3.4 Hz, 1H), 5.07 (s, 2H), 4.73 – 4.44 (m, 1H), 3.75 (s, 2H), 3.65 (br s, 1H), 3.60 – 3.40 (m, 5H), 3.37 – 3.20 (m, 3H), 1.65 (br s, 1H), 1.62 – 1.46 (m, 2H), 1.42 – 1.28 (m, 2H); ^{13}C NMR (100 MHz, $CDCl_3$) δ 171.0, 170.2, 166.0, 156.6, 136.7, 135.0, 131.3, 129.4, 129.0, 128.9, 128.7, 128.5, 127.6, 126., 67.5, 50.7, 46.5, 46.1, 45.7, 42.4, 41.7, 41.5, 39.4, 33.3, 29.3, 22.6; HRMS (ESI-QTOF) m/z [M + Na]+ calcd for $C_{29}H_{36}N_4O_5Na$ 543.2583; found 543.2587.

(S)-benzyl(1-(4-acetylpiperazin-1-yl)-5-acrylamido-1-oxopentan-2-yl)carbamate (**53**)

Compound **53** was prepared from Boc-deprotected **44** and compound **1** using General Procedure A to collect 36 mg (21 %) of the desired product as a clear oil. ^{1}H NMR (400 MHz, $CDCl_3$) δ 7.37 – 7.28 (m, 5H), 6.27 – 6.22 (d, *J* = 17.0, 1H), 6.10 – 6.03 (dd, *J* = 10.2, 17.0 Hz, 1H), 5.99 (s, 1H), 5.83 – 5.81 (d, *J* = 8.3 Hz, 1H), 5.61 – 5.58 (d, *J* = 10.2 Hz, 1H), 5.07 (s, 2H), 4.62 (s,

1H), 3.78 – 3.69 (m, 2H), 3.63 – 3.43 (m, 6H), 3.36 – 3.30 (m, 2H), 2.10 (s, 3H), 1.68 (s, 1H), 1.61-1.54 (m, 3H), 1.42-1.31 (m, 2H); ^{13}C NMR (100 MHz, $CDCl_3$) δ 170.7, 170.5, 169.3, 169.2, 165.7, 156.2, 136.2, 130.9, 128.5, 128.2, 128.0, 126.3, 67.0, 50.3, 46.2, 45.8, 45.5, 45.2, 41.9, 41.3, 41.0, 39.0, 38.8, 32.8, 32.7, 28.9, 22.2, 21.3; HRMS (ESI-TOF) m/z [M + Na]+ calcd for $C_{23}H_{32}N_4O_5Na$ 467.2270; found 467.2300.

(S)-benzyl(6-acrylamido-1-oxo-1-(4-picolinoylpiperazin-1-yl)hexan-2-yl)carbamate (**54**). Compound **54** was prepared from Boc-deprotected **45** and compound **1** using General Procedure A to collect 17 mg (10 %) of the desired product as a colorless oil. ^{1}H NMR (300 MHz, $(CD_3)_2SO$ at 80 ˚C) δ 8.60 (d, *J* = 4.6 Hz, 1H), 7.93 (td, *J* = 7.7, 1.8 Hz, 1H), 7.76 (br s, 1H), 7.61 (d, *J* = 7.8 Hz, 1H), 7.48 (ddd, *J* = 7.6, 4.8, 1.2 Hz, 1H), 7.38 – 7.31 (m, 5H), 7.08 (br s, 1H), 6.20 (dd, *J* = 17.1, 10.0 Hz, 1H), 6.04 (dd, *J* = 17.1, 2.4 Hz, 1H), 5.52 (dd, *J* = 10.0, 2.4 Hz, 1H), 5.04 (s, 2H), 4.55 – 4.29 (m, 1H), 3.57 (br s, 8H), 3.18 – 3.08 (m, 2H), 1.68 – 1.58 (m, 2H), 1.53 – 1.40 (m, 2H), 1.40 – 1.23 (m, 1H), ^{13}C NMR (75 MHz, $(CD_3)_2SO$ at 80 ˚C) δ 170.1, 166.5, 164.2, 153.4, 147.9, 136.8, 136.7, 131.7, 127.8, 127.2, 127.1, 124.2, 123.8, 122.8, 65.2, 50.4, 37.9, 30.0, 28.4, 22.2; HRMS (ESI-QTOF) m/z $[M + Na]^+$ calcd for $C_{27}H_{33}N_5NaO_5$ 530.2379; found 530.2347.

(S)-benzyl (6-acrylamido-1-(4-nicotinoylpiperazin-1-yl)-1-oxohexan-2-yl)carbamate (**55**). Compound **55** was prepared from Boc-deprotected **46** and compound **1** using General Procedure A to collect 25 mg (14 %) of the desired product as a clear, colorless oil. ^{1}H NMR (300 MHz, $(CD_3)_2SO$ at 120 ˚C) δ 8.70 – 8.60 (m, 1H), 7.86 – 7.77 (m, 1H), 7.46 (dd, *J* = 7.9, 4.8 Hz, 1H), 7.41 – 7.22 (m, 5H), 6.79 (bs, 1H), 6.20 (dd, *J* = 17.2, 10.1 Hz, 1H), 6.04 (dd, *J* = 17.2, 2.4 Hz, 1H), 5.51 (dd, *J* = 10.1, 2.4 Hz, 1H), 5.06 (s, 2H), 4.51-4.42 (m, 1H), 3.62-3.54 (m, 4H), 3.53.48 (d, 4H), 3.15 (q, *J* = 6.5 Hz, 2H), 1.71-1.58 (m, *J* = 14.3, 7.6 Hz, 2H), 1.52-1.44 (m, *J* = 6.8 Hz,

2H), 1.40-1.32 (m, *J* = 8.4, 7.8 Hz, 1H), ^{13}C NMR (75 MHz, $(CD_3)_2SO$ at 120 ˚C) δ 169.9, 166.6, 164.2, 155.0, 149.7, 147.0, 136.5, 133.9, 131.7, 131.0, 127.5, 126.9, 126.82, 123.1, 122.6, 65.1, 50.2, 43.7, 37.8, 30.8, 28.2, 21.9; HRMS (ESI-QTOF) m/z $[M + Na]^+$ calcd for $C_{27}H_{33}N_5O_5Na$ 530.2379; found 530.2396.

(S)-benzyl-(6-acrylamido-1-(4-isonicotinoylpiperazin-1-yl)-1-oxohexan-2-yl)carbamate (**56**). Compound **56** was prepared from Boc-deprotected **47** and compound **1** using General Procedure A to collect 40 mg (22 %) of the desired product as a clear, colorless oil. ^{1}H NMR (300 MHz, $(CD_3)_2SO$ at 80 ˚C) δ 8.68 (d, *J* = 6.0 Hz, 2H), 7.76 (br s, 1H), 7.38 (d, *J* = 5.9 Hz, 2H), 7.36 – 7.27 (m, 5H), 7.07 (bs, 1H), 6.20 (dd, *J* = 17.2, 10.0 Hz, 1H), 6.04 (dd, *J* = 17.2, 2.5 Hz, 1H), 5.52 (dd, *J* = 10.0, 2.5 Hz, 1H), 5.04 (s, 2H), 4.43 (td, *J* = 8.0, 5.3 Hz, 1H), 3.73 – 3.34 (m, 8H), 3.12 (q, *J* = 6.5 Hz, 2H), 1.70 – 1.54 (m, 2H), 1.49 – 1.40 (m, 2H), 1.38 – 1.27 (m, 2H), ^{13}C NMR (75 MHz, $(CD_3)_2SO$ at 80 ˚C) δ 170.1, 166.7, 164.2, 155.3, 149.6, 142.8, 136.7, 131.7, 127.8, 127.3, 127.1, 123.8, 120.7, 65.2, 50.3, 37.9, 30.8, 28.4, 22.2; HRMS (ESI-QTOF) m/z $[M + Na]^+$ calcd for $C_{27}H_{33}N_5NaO_5$ 530.2379; found 530.2370.

(S)-benzyl(6-acrylamido-1-(4-(7-hydroxy-2-oxo-2H-chromene-3-carbonyl)piperazin-1-yl)-1-oxohexan-2-yl)carbamate (**57 aka VA5**). Compound **57** was prepared according to our recently published synthesis (same as **13**).[60] HR MS (ESI-QTOF) m/z $[M + Na]^+$ calcd for $C_{31}H_{34}N_4O_8Na$ 613.2274; found 613.2282.

ASSOCIATED CONTENT

Supporting Information. Additional synthetic methods and supplemental compound characterization data (NMR, HPLC), kinetic inhibition and selectivity data, K_M values for substrate AL5 with TGase isoforms hTG1, hTG2, hTG3, hTG6 and FXIIIa. The following files are available free of charge: Supporting Information (PDF), Molecular Formula Strings (CSV).

AUTHOR INFORMATION

Corresponding Author

jkeillor@uottawa.ca

Author Contributions

The manuscript was written through contributions from AA, NMRM and JWK. All authors have given approval to the final version of the manuscript. ‡These authors contributed equally.

ACKNOWLEDGMENTS

This work was financially supported by the University of Ottawa in the form of a University Research Chair (JWK) and by the Natural Sciences and Engineering Research Council of Canada (NSERC) in the form of a Discovery Grant (JWK). NMRM and MRA are also grateful to NSERC for postdoctoral and undergraduate scholarships, respectively. The authors are also very grateful to Dr. Martin Hils (Zedira) for measurement of K_M values of **A101** with various TGases.

ABBREVIATIONS

hTG2, human transglutaminase 2; TGase, transglutaminase; hFXIIIa, activated human factor XIII; hTG1, human keratinocyte transglutaminase; hTG3a, activated human epidermal transglutaminase; hTG6, human neuronal transglutaminase; gplTG2, guinea pig liver transglutaminase; EMC, extracellular matrix; TIC, targeted-covalent inhibitors; pNP, p-nitrophenolate; SAR, structure-activity relationship; ACR, acrylamide; ECS, epidermal cancer stem cells; EMT, epithelial-mesenchymal transition; BODIPY, boron-dipyrromethene difluoride; NHS, N-hydroxysuccinimide; EDC, 1-Ethyl-3-(3-dimethylaminopropyl)carbodiimide; LiOH, lithium hydroxide; HOBt, hydroxybenzotriazole; GTPγS, guanosine 5'-O-(3-thiotriphosphate); QTOF, quadrupole time-of-flight; ACN, acetonitrile; DMSO, dimethyl sulfoxide.

REFERENCES

1. Gundemir, S.; Colak, G.; Tucholski, J.; Johnson, G. V. W. Transglutaminase 2: A molecular Swiss army knife. *Biochim. Biophys. Acta, Mol. Cell Res.* **2012,** *1823* (2), 406-419.

2. Eckert, R. L.; Kaartinen, M. T.; Nurminskaya, M.; Belkin, A. M.; Colak, G.; Johnson, G. V. W.; Mehta, K. Transglutaminase regulation of cell function. *Physiol. Rev.* **2014,** *94* (2), 383-417.

3. Chen, J. S. K.; Mehta, K. Tissue transglutaminase: an enzyme with a split personality. *Int. J. Biochem. Cell Biol.* **1999,** *31* (8), 817-836.

4. Di Venere, A.; Rossi, A.; De Matteis, F.; Rosato, N.; Agro, A. F.; Mei, G. Opposite effects of Ca^{2+} and GTP binding on tissue transglutaminase tertiary structure. *J. Biol. Chem.* **2000,** *275* (6), 3915-3921.

5. Klöck, C.; Khosla, C. Regulation of the activities of the mammalian transglutaminase family of enzymes. *Protein Sci.* **2012,** *21* (12), 1781-1791.

6. Stamnaes, J.; Pinkas, D. M.; Fleckenstein, B.; Khosla, C.; Sollid, L. M. Redox regulation of transglutaminase 2 activity. *J. Biol. Chem.* **2010,** *285* (33), 25402-25409.

7. Folk, J. E.; Cole, P. W. Identification of a functional cysteine essential for the activity of guinea pig liver transglutaminase. *J. Biol. Chem.* **1966,** *241* (13), 3238-3240.

8. Pinkas, D. M.; Strop, P.; Brunger, A. T.; Khosla, C. Transglutaminase 2 undergoes a large conformational change upon activation. *PLoS Biol.* **2007,** *5* (12), 2788-2796.

9. Liu, S.; Cerione, R. A.; Clardy, J. Structural basis for the guanine nucleotide-binding activity of tissue transglutaminase and its regulation of transamidation activity. *Proc. Natl. Acad. Sci.* **2002,** *99* (5), 2743-2747.

10. Keillor, J. W.; Clouthier, C. M.; Apperley, K. Y. P.; Akbar, A.; Mulani, A. Acyl transfer mechanisms of tissue transglutaminase. *Bioorg. Chem.* **2014,** *57*, 186-197.

11. Chica, R. A.; Gagnon, P.; Keillor, J. W.; Pelletier, J. N. Tissue transglutaminase acylation: proposed role of conserved active site Tyr and Trp residues revealed by molecular modeling of peptide substrate binding. *Protein Sci.* **2004,** *13* (4), 979-991.

12. Caron, N. S.; Munsie, L. N.; Keillor, J. W.; Truant, R. Using FLIM-FRET to measure conformational changes of transglutaminase type 2 in live cells. *PLoS One.* **2012,** *7* (8), e44159.

13. Kanchan, K.; Fuxreiter, M.; Fésüs, L. Physiological, pathological, and structural implications of non-enzymatic protein–protein interactions of the multifunctional human transglutaminase 2. *Cell. Mol. Life Sci.* **2015,** *72* (16), 3009-3035.

14. Keillor, J. W. Inhibition of Transglutaminase. In *Transglutaminases: Multiple Functional Modifiers and Targets for New Drug Discovery*, Hitomi, K.; Kojima, S.; Fesus, L., Eds.; Springer: Tokyo, Japan, 2015; pp 347-372.

15. Tatsukawa, H.; Furutani, Y.; Hitomi, K.; Kojima, S. Transglutaminase 2 has opposing roles in the regulation of cellular functions as well as cell growth and death. *Cell Death Dis.* **2016,** *7*, e2244.

16. Haroon Z.A., W. T., Gupta M., Greenberg C.S., Wallin R., Sane D.C. Localization of tissue transglutaminase in human carotid and coronary artery atherosclerosis: implications for plaque stability and progression. *Lab. Invest.* **2001,** *81* (1), 83-93.

17. Olsen, K. C.; Epa, A. P.; Kulkarni, A. A.; Kottmann, R. M.; McCarthy, C. E.; Johnson, G. V.; Thatcher, T. H.; Phipps, R. P.; Sime, P. J. Inhibition of transglutaminase 2, a novel target for pulmonary fibrosis, by two small electrophilic molecules. *Am. J. Respir. Cell Mol. Biol.* **2014,** *50* (4), 737-747.

18. Iismaa, S. E.; Mearns, B. M.; Lorand, L.; Graham, R. M. Transglutaminases and disease: lessons from genetically engineered mouse models and inherited disorders. *Physiol. Rev.* **2009,** *89* (3), 991-1023.

19. Daneshpour, N.; Griffin, M.; Collighan, R.; Perrie, Y. Targeted delivery of a novel group of site-directed transglutaminase inhibitors to the liver using liposomes: a new approach for the potential treatment of liver fibrosis. *J. Drug Targeting* **2011,** *19* (8), 624-631.

20. Kuo, T.-F.; Tatsukawa, H.; Matsuura, T.; Nagatsuma, K.; Hirose, S.; Kojima, S. Free fatty acids induce transglutaminase 2-dependent apoptosis in hepatocytes via ER stress-stimulated PERK pathways. *J. Cell. Physiol.* **2012,** *227* (3), 1130-1137.

21. Scarpellini, A.; Huang, L.; Burhan, I.; Schroeder, N.; Funck, M.; Johnson, T. S.; Verderio, E. A. M. Syndecan-4 knockout leads to reduced extracellular transglutaminase-2 and protects against tubulointerstitial fibrosis. *J. Am. Soc. Nephrol.* **2014,** *25* (5), 1013-1027.

22. Wilhelmus, M. M. M.; de Jager, M.; Smit, A. B.; van der Loo, R. J.; Drukarch, B. Catalytically active tissue transglutaminase colocalises with Aβ pathology in Alzheimer's disease mouse models. *Sci. Rep.* **2016,** *6:20569*.

23. Dieterich, W.; Ehnis, T.; Bauer, M.; Donner, P.; Volta, U.; Riecken, E. O.; Schuppan, D. Identification of tissue transglutaminase as the autoantigen of celiac disease. *Nat. Med.* **1997,** *3* (7), 797-801.

24. Fleckenstein, B.; Molberg, O.; Qiao, S.-W.; Schmid, D. G.; von der Mulbe, F.; Elgstoen, K.; Jung, G.; Sollid, L. M. Gliadin T cell Epitope selection by tissue transglutaminase in celiac disease. Role of enzyme specificity and pH influence on the transamidation versus deamidation reactions. *J. Biol. Chem.* **2002,** *277* (37), 34109-34116.

25. Giersiepen, K.; Lelgemann, M.; Stuhldreher, N.; Ronfani, L.; Husby, S.; Koletzko, S.; Korponay-Szabo, I. R. Accuracy of diagnostic antibody tests for coeliac disease in children: Summary of an evidence report. *J. Pediatr. Gastroenterol. Nutr.* **2012,** *54* (2), 229-241.

26. Nadalutti, C. A.; Korponay-Szabo, I. R.; Kaukinen, K.; Griffin, M.; Maki, M.; Lindfors, K. Celiac disease patient IgA antibodies induce endothelial adhesion and cell polarization defects via extracellular transglutaminase 2. *Cell. Mol. Life Sci.* **2014,** *71* (7), 1315-1326.

27. Eckert, R. L.; Fisher, M. L.; Grun, D.; Adhikary, G.; Xu, W.; Kerr, C. Transglutaminase is a tumor cell and cancer stem cell survival factor. *Mol. Carcinog.* **2015,** *54* (10), 947-958.

28. Fisher, M. L.; Adhikary, G.; Xu, W.; Kerr, C.; Keillor, J. W.; Eckert, R. L. Type II transglutaminase stimulates epidermal cancer stem cell epithelial-mesenchymal transition. *Oncotarget* **2015,** *6* (24), 20525-20539.

29. Fisher, M. L.; Keillor, J. W.; Xu, W.; Eckert, R. L.; Kerr, C. Transglutaminase is required for epidermal squamous cell carcinoma stem cell survival. *Mol. Cancer Res.* **2015,** *13* (7), 1083-1094.

30. Kerr, C.; Szmacinski, H.; Fisher, M. L.; Nance, B.; Lakowicz, J. R.; Akbar, A.; Keillor, J. W.; Lok Wong, T.; Godoy-Ruiz, R.; Toth, E. A.; Weber, D. J.; Eckert, R. L. Transamidase site-targeted agents alter the conformation of the transglutaminase cancer stem cell survival protein to reduce GTP binding activity and cancer stem cell survival. *Oncogene* **2017,** *36* (21), 2981-2990.

31. Fisher, M. L.; Kerr, C.; Adhikary, G.; Grun, D.; Xu, W.; Keillor, J. W.; Eckert, R. L. Transglutaminase interaction with α6/β4-Integrin stimulates YAP1-dependent ΔNp63α stabilization and leads to enhanced cancer stem cell survival and tumor formation. *Cancer Res.* **2016,** *76* (24), 7265-7276.

32. Sarang, Z.; Tóth, B.; Balajthy, Z.; Köröskényi, K.; Garabuczi, É.; Fésüs, L.; Szondy, Z. Some lessons from the tissue transglutaminase knockout mouse. *Amino Acids* **2008,** *36* (4), 625-631.

33. Pietsch, M.; Wodtke, R.; Pietzsch, J.; Loeser, R. Tissue transglutaminase: An emerging target for therapy and imaging. *Bioorg. Med. Chem. Lett.* **2013,** *23* (24), 6528-6543.

34. Agnihotri, N.; Mehta, K. Transglutaminase-2: evolution from pedestrian protein to a promising therapeutic target. *Amino Acids* **2016**, 1-15.

35. Keillor, J. W.; Apperley, K. Y. P.; Akbar, A. Inhibitors of tissue transglutaminase. *Trends Pharmacol. Sci.* **2015,** *36* (1), 32-40.

36. Song, M.; Hwang, H.; Im, C. Y.; Kim, S.-Y. Recent progress in the development of transglutaminase 2 (TGase2) inhibitors. *J. Med. Chem.* **2017,** *60* (2), 554-567.

37. Keillor, J. W.; Apperley, K. Y. P. Transglutaminase inhibitors: a patent review. *Expert Opin. Ther. Pat.* **2016,** *26* (1), 49-63.

38. Apperley, K. Y. P.; Roy, I.; Saucier, V.; Brunet-Filion, N.; Piscopo, S.-P.; Pardin, C.; De Francesco, E.; Hao, C.; Keillor, J. W. Development of new scaffolds as reversible tissue transglutaminase inhibitors, with improved potency or resistance to glutathione addition. *MedChemComm* **2017,** *8*, 338-345.

39. Griffin, M.; Mongeot, A.; Collighan, R.; Saint, R. E.; Jones, R. A.; Coutts, I. G. C.; Rathbone, D. L. Synthesis of potent water-soluble tissue transglutaminase inhibitors. *Bioorg. Med. Chem. Lett.* **2008,** *18* (20), 5559-5562.

40. Choi, K.; Siegel, M.; Piper, J. L.; Yuan, L.; Cho, E.; Strnad, P.; Omary, B.; Rich, K. M.; Khosla, C. Chemistry and biology of dihydroisoxazole derivatives: Selective inhibitors of human transglutaminase 2. *Chem. Biol.* **2005,** *12* (4), 469-475.

41. Zedira-GmbH. Michael Systems as Transglutaminase Inhibitors. U.S. Patent 8471063. 2013.

42. Marrano, C.; de Macedo, P.; Keillor, J. W. Evaluation of novel dipeptide-bound α,β-unsaturated amides and epoxides as irreversible inhibitors of guinea pig liver transglutaminase. *Bioorg. Med. Chem.* **2001,** *9* (7), 1923-1928.

43. de Macedo, P.; Marrano, C.; Keillor, J. W. Synthesis of dipeptide-bound epoxides and α,β-unsaturated amides as potential irreversible transglutaminase inhibitors. *Bioorg. Med. Chem.* **2001,** *10* (2), 355-360.

44. Prime, M. E.; Andersen, O. A.; Barker, J. J.; Brooks, M. A.; Cheng, R. K. Y.; Toogood-Johnson, I.; Courtney, S. M.; Brookfield, F. A.; Yarnold, C. J.; Marston, R. W.; Johnson, P. D.; Johnsen, S. F.; Palfrey, J. J.; Vaidya, D.; Erfan, S.; Ichihara, O.; Felicetti, B.; Palan, S.; Pedret-Dunn, A.; Schaertl, S.; Sternberger, I.; Ebneth, A.; Scheel, A.; Winkler, D.; Toledo-Sherman, L.; Beconi, M.; Macdonald, D.; Munoz-Sanjuan, I.; Dominguez, C.; Wityak, J. Discovery and structure-activity relationship of potent and selective covalent inhibitors of transglutaminase 2 for Huntington's disease. *J. Med. Chem.* **2012,** *55* (3), 1021-1046.

45. Prime, M. E.; Brookfield, F. A.; Courtney, S. M.; Gaines, S.; Marston, R. W.; Ichihara, O.; Li, M.; Vaidya, D.; Williams, H.; Pedret-Dunn, A.; Reed, L.; Schaertl, S.; Toledo-Sherman, L.; Beconi, M.; Macdonald, D.; Munoz-Sanjuan, I.; Dominguez, C.; Wityak, J. Irreversible 4-aminopiperidine transglutaminase 2 inhibitors for Huntington's disease. *ACS Med. Chem. Lett.* **2012,** *3* (9), 731-735.

46. Wityak, J.; Prime, M. E.; Brookfield, F. A.; Courtney, S. M.; Erfan, S.; Johnsen, S.; Johnson, P. D.; Li, M.; Marston, R. W.; Reed, L.; Vaidya, D.; Schaertl, S.; Pedret-Dunn, A.; Beconi, M.; MacDonald, D.; Munoz-Sanjuan, I.; Dominguez, C. SAR development of lysine-

based irreversible inhibitors of transglutaminase 2 for Huntington's disease. *ACS Med. Chem. Lett.* **2012,** *3* (12), 1024-1028.

47. Badarau, E.; Wang, Z.; Rathbone, D. L.; Costanzi, A.; Thibault, T.; Murdoch, C. E.; El Alaoui, S.; Bartkeviciute, M.; Griffin, M. Development of potent and selective tissue transglutaminase inhibitors: Their effect on TG2 function and application in pathological conditions. *Chem. Biol.* **2015,** *22* (10), 1347-1361.

48. Keillor, J. W.; Chabot, N.; Roy, I.; Mulani, A.; Leogane, O.; Pardin, C. Irreversible inhibitors of tissue transglutaminase. *Adv. Enzymol. Relat. Areas Mol. Biol.* **2011,** *78*, 415-447.

49. Baillie, T. A. Targeted covalent inhibitors for drug design. *Angew. Chem. Int. Ed.* **2016,** *55* (43), 13408-13421.

50. Keillor, J. W. Tissue transglutaminase inhibition. *Chem. Biol.* **2005,** *12* (4), 410-412.

51. Keillor, J. W.; Chica, R. A.; Chabot, N.; Vinci, V.; Pardin, C.; Fortin, E.; Gillet, S. M. F. G.; Nakano, Y.; Kaartinen, M. T.; Pelletier, J. N.; Lubell, W. D. The bioorganic chemistry of transglutaminase - from mechanism to inhibition and engineering. *Can. J. Chem.* **2008,** *86* (4), 271-276.

52. Pardin, C.; Gillet, S. M. F. G.; Keillor, J. W. Synthesis and evaluation of peptidic irreversible inhibitors of tissue transglutaminase. *Bioorg. Med. Chem.* **2006,** *14* (24), 8379-8385.

53. Jackson, P. A.; Widen, J. C.; Harki, D. A.; Brummond, K. M. Covalent modifiers: A chemical perspective on the reactivity of α,β-unsaturated carbonyls with thiols via hetero-Michael addition reactions. *J. Med. Chem.* **2017,** *60* (3), 839-885.

54. Valeur, E.; Bradley, M. Amide bond formation: beyond the myth of coupling reagents. *Chem. Soc. Rev.* **2009,** *38* (2), 606-631.

55. Leblanc, A.; Gravel, C.; Labelle, J.; Keillor, J. W. Kinetic studies of guinea pig liver transglutaminase reveal a general-base-catalyzed deacylation mechanism. *Biochemistry* **2001,** *40* (28), 8335-8342.

56. Kitz, R.; Wilson, I. B. Esters of methanesulfonic acid as irreversible inhibitors of acetylcholinesterase. *J. Biol. Chem.* **1962,** *237*, 3245-3249.

57. Lipinski, C. A.; Lombardo, F.; Dominy, B. W.; Feeney, P. J. Experimental and computational approaches to estimate solubility and permeability in drug discovery and development settings. *Adv. Drug Delivery Rev.* **1997,** *23* (1-3), 3-25.

58. Veber, D. F.; Johnson, S. R.; Cheng, H.-Y.; Smith, B. R.; Ward, K. W.; Kopple, K. D. Molecular properties that influence the oral bioavailability of drug candidates. *J. Med. Chem.* **2002,** *45* (12), 2615-2623.

59. Mironov, G. G.; Clouthier, C. M.; Akbar, A.; Keillor, J. W.; Berezovski, M. V. Simultaneous analysis of enzyme structure and activity by kinetic capillary electrophoresis-MS. *Nat. Chem. Biol.* **2016,** *12* (11), 918-922.

60. Gundemir, S.; Monteagudo, A.; Akbar, A.; Keillor, J. W.; Johnson, G. V. W. The complex role of transglutaminase 2 in glioblastoma proliferation. *Neuro-Oncology* **2017,** *19* (2), 208-218.

61. Clouthier, C. M.; Mironov, G. G.; Okhonin, V.; Berezovski, M. V.; Keillor, J. W. Real-time monitoring of protein conformational dynamics in solution using kinetic capillary electrophoresis. *Angew. Chem., Int. Ed.* **2012,** *51* (50), 12464-12468.

62. McEwen, D. P.; Gee, K. R.; Kang, H. C.; Neubig, R. R. Fluorescent BODIPY-GTP analogs: Real-time measurement of nucleotide binding to G proteins. *Anal. Biochem.* **2001,** *291* (1), 109-117.

63. Barsigian, C.; Stern, A. M.; Martinez, J. Tissue (type II) transglutaminase covalently incorporates itself, fibrinogen, or fibronectin into high molecular weight complexes on the extracellular surface of isolated hepatocytes. Use of 2-[(2-oxopropyl)thio] imidazolium derivatives as cellular transglutaminase inactivators. *J. Biol. Chem.* **1991,** *266* (33), 22501-22509.

64. Freund, K. F.; Doshi, K. P.; Gaul, S. L.; Claremon, D. A.; Remy, D. C.; Baldwin, J. J.; Pitzenberger, S. M.; Stern, A. M. Transglutaminase inhibition by 2-[(2-oxopropyl)thio]imidazolium derivatives: Mechanism of factor XIIIa inactivation. *Biochemistry* **1994,** *33* (33), 10109-10119.

65. Balklava, Z.; Verderio, E.; Collighan, R.; Gross, S.; Adams, J.; Griffin, M. Analysis of tissue transglutaminase function in the migration of Swiss 3T3 fibroblasts: The active-state conformation of the enzyme does not affect cell motility but is important for its secretion. *J. Biol. Chem.* **2002,** *277* (19), 16567-16575.

66. Oertel, K.; Hunfeld, A.; Specker, E.; Reiff, C.; Seitz, R.; Pasternack, R.; Dodt, J. A highly sensitive fluorometric assay for determination of human coagulation factor XIII in plasma. *Anal. Biochem.* **2007,** *367* (2), 152-158.

67. Király, R.; Thangaraju, K.; Nagy, Z.; Collighan, R.; Nemes, Z.; Griffin, M.; Fésüs, L. Isopeptidase activity of human transglutaminase 2: disconnection from transamidation and characterization by kinetic parameters. *Amino Acids* **2016,** *48* (1), 31-40.

68. Copeland, R. A. *Evaluation of Enzyme Inhibitors in Drug Discovery: A Guide for Medicinal Chemists and Pharmacologists*. John Wiley & Sons, Inc: Hoboken, NJ, USA, 2013; pp 345–382.

69. Adhikary, G. G., D.; Kerr, C.; Balasubramanian, S.; Rorke, E. A.; Vemuri, M.; Boucher, S.; Bickenbach, J. R.; Hornyak, T.; Xu, W.; Fisher, M. L.; Eckert, R. L. Identification of a population of epidermal squamous cell carcinoma cells with enhanced potential for tumor formation. *PLoS One.* **2013,** *8*, e84324.

70. Stone, S. R.; Hofsteenge, J. Specificity of activated human protein C. *Biochem. J.* **1985,** *230* (2), 497-502.

71. Adhikary, G.; Grun, D.; Balasubramanian, S.; Kerr, C.; Huang, J. M.; Eckert, R. L. Survival of skin cancer stem cells requires the Ezh2 polycomb group protein. *Carcinogenesis* **2015,** *36* (7), 800-810.

72. Gobbo, P.; Gunawardene, P.; Luo, W.; Workentin, M. S. Synthesis of a toolbox of clickable rhodamine B derivatives. *Synlett* **2015,** *26* (09), 1169-1174.

For Table of Contents Only

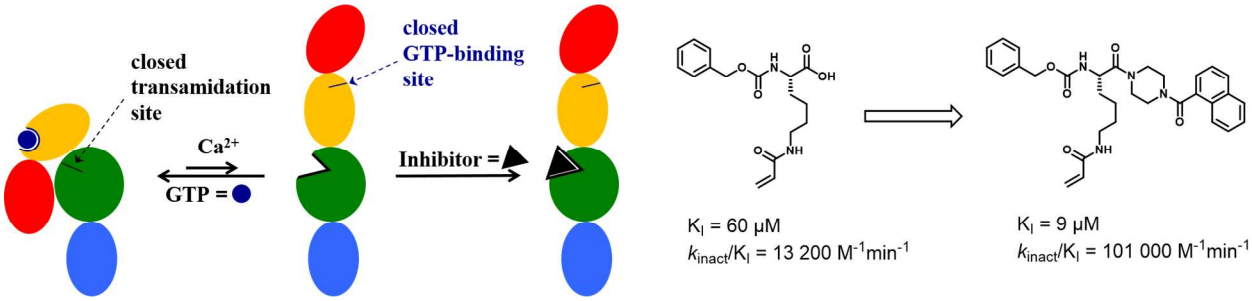

Keywords

tissue transglutaminase, targeted covalent inhibitor, acrylamide, transamidation, GTP-binding